AD-A110 340 VARIAN ASSOCIATES INC PALO ALTO CA PALO ALTO MICROWA--ETC F/G 9/1
HIGH EFFICIENCY AMPLIFIER.(U)
OCT 81 W R AYERS, R H GIEBELER F30602-80-C-0052
UNCLASSIFIED RADC-TR-81-288 NL

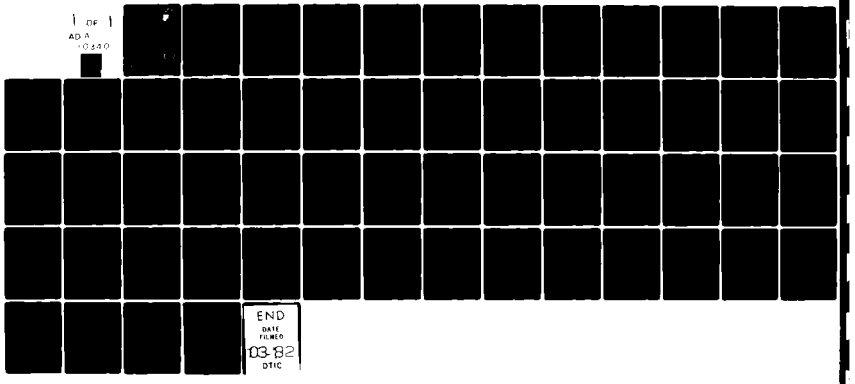

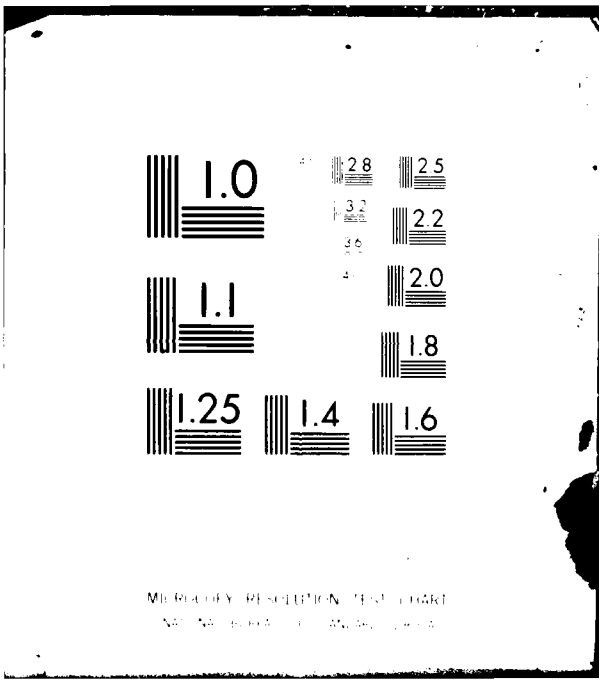
1.0
2.8
2.5
3.2
2.2
3.6
4.0
2.0
1.1
1.8
1.25
1.4
1.6

LEVEL II

12

RADC-TR-81-288
Final Technical Report
October 1981

HIGH EFFICIENCY AMPLIFIER

Varian Associates, Inc.

W. R. Ayers
R. H. Giebeler
L. R. Veselovsky
F. Ruth Walker

ROME AIR DEVELOPMENT CENTER
Air Force Systems Command
Griffiss Air Force Base, New York 13441

This report has been reviewed by the RADC Public Affairs Office (PA) and is releasable to the National Technical Information Service (NTIS). At NTIS it will be releasable to the general public, including foreign nations.

RADC-TR-81-288 has been reviewed and is approved for publication.

APPROVED:

JOSEPH J. POLNIASZEK
Project Engineer

APPROVED:

FRANK J. REHM
Technical Director
Surveillance Division

FOR THE COMMANDER:

JOHN P. HUSS
Acting Chief, Plans Office

If your address has changed or if you wish to be removed from the RADC mailing list, or if the addressee is no longer employed by your organization, please notify RADC (OCTP) Griffiss AFB NY 13441. This will assist us in maintaining a current mailing list.

Do not return copies of this report unless contractual obligations or notices on a specific document requires that it be returned.

UNCLASSIFIED

SECURITY CLASSIFICATION OF THIS PAGE (When Data Entered)

REPORT DOCUMENTATION PAGE		READ INSTRUCTIONS BEFORE COMPLETING FORM
1. REPORT NUMBER RADC-TR-81-288	2. GOVT ACCESSION NO. AD-A110340	3. RECIPIENT'S CATALOG NUMBER
4. TITLE (and Subtitle) HIGH EFFICIENCY AMPLIFIER		5. TYPE OF REPORT & PERIOD COVERED Final Technical Report Oct 79 - Sep 81
		6. PERFORMING ORG. REPORT NUMBER N/A
7. AUTHOR(s) W. R. Ayers L. R. Veselovsky R. H. Giebeler F. Ruth Walker		8. CONTRACT OR GRANT NUMBER(s) F30602-80-C-0052
9. PERFORMING ORGANIZATION NAME AND ADDRESS Varian Associates, Inc. 611 Hansen Way Palo Alto CA 94303		10. PROGRAM ELEMENT, PROJECT, TASK AREA & WORK UNIT NUMBERS 62702F 45061255
11. CONTROLLING OFFICE NAME AND ADDRESS Rome Air Development Center (OCTP) Griffiss AFB NY 13441		12. REPORT DATE October 1981 13. NUMBER OF PAGES 48
14. MONITORING AGENCY NAME & ADDRESS(if different from Controlling Office) Same		15. SECURITY CLASS. (of this report) UNCLASSIFIED 15a. DECLASSIFICATION/DOWNGRADING SCHEDULE N/A

16. DISTRIBUTION STATEMENT (of this Report)

Approved for public release; distribution unlimited.

17. DISTRIBUTION STATEMENT (of the abstract entered in Block 20, if different from Report)

Same

18. SUPPLEMENTARY NOTES

RADC Project Engineer: Joseph Polniaszek (OCTP)

19. KEY WORDS (Continue on reverse side if necessary and identify by block number)

Traveling Wave Tubes
Efficiency
Coupled Cavity
Microwave Power Devices
Linear Beam Tubes

20. ABSTRACT (Continue on reverse side if necessary and identify by block number)

An exploratory development model was designed, constructed and evaluated. The design followed the criterion set forth in efficiency improvements in Coupled Cavity TWTs (F30602-78-C-0117) with the exception of a confined flow beam instead of brilluoin focusing.

The results exceeded all performance parameters except interaction efficiency. Electronic efficiency, however was found to be 45% with 33%

DD FORM 1 JAN 73 1473 EDITION OF 1 NOV 65 IS OBSOLETE

UNCLASSIFIED

SECURITY CLASSIFICATION OF THIS PAGE (When Data Entered)

depression of a standard single stage collector. The measured interaction efficiency agreed well with predicted efficiency. Bandwidth of 500 MHz with .5db maximum variation was displayed and very low ripple in both amplitude and phase. Tube stability was excellent.

PREFACE

The work described herein was done by Barian Associates, Inc., Palo Alto Microwave Tube Division under RADC Contract F30602-80-C-0052 with R.H. Giebeler as principal investigator. Others contributing to the project included W.R. Ayers, E.C. Brum, J.S. Lawton, G.V. Miram, J.A. Ruet, L.R. Veselovsky and R. Walker. Mr. Joseph Polniaszek, Rome Air Development Center, was Project Manager.

TABLE OF CONTENTS

LIST OF ILLUSTRATIONS

BLANK PAGE

1.0 INTRODUCTION

1.1 Objective, Background, and Scope

The objective of this program was to design, develop, fabricate, test and evaluate a high power coupled-cavity TWT with conversion efficiency of 40 percent. This design was to be based upon the efficiency optimizing techniques developed under contract F30602-78-C-0117.

In order to maximize the useful results, the effort was to focus upon the output section of the TWT using, wherever practical, existing designs and parts from similar TWTs for the drive sections, focusing solenoid, collector and output windows. A new Brillouin flow gun was to be developed since it had been predicted that confined flow focusing was detrimental to efficiency; however, technical difficulties prevented its use and a standard confined flow gun was used.

1.2 Synopsis of Report

This report is organized chronologically. Section 2 deals with the specifications and performance objective which form the basis for this work.

Section 3 describes how the TWT was developed, starting with the design concepts of contract F30602-78-C-0117. Cold test results are shown and the parameters for the final design are developed.

Section 4 details the test results, including tests carried out over a wide range of voltages, frequencies, currents and duty cycles. The analysis of the test results leads to a number of useful conclusions and recommendations for future work, which are presented in Section 5.

2.0 PERFORMANCE OBJECTIVES

The specific design goals for the experimental breadboard TWT are as follows:

Frequency Band	3.1 to 3.6 GHz
Electronic Bandwidth	500 MHz Flat within 1 dB
Peak Power	100 KW
Average Power	10 KW
Duty Factor	10% Minimum
Pulse Width	10 to 300 μSeconds
Gain	40 dB Minimum
Conversion Efficiency	40% Minimum

This TWT is to be an Exploratory Development Model; an item (preliminary parts or circuits) used for experimentation or tests to investigate or evaluate the feasibility and practicality of a concept, device, circuits, or system in breadboard or rough experimental form, without regard to the eventual overall fit or final form.

3.0 TWT DESIGN

3.1 Introduction

The work in this section follows very closely the final design developed under contract F30602-78-C-0117 and described in Chapter 6 of RADC-TR-79-264.

3.2 Output Circuit

The High Efficiency S-Band TWT is shown schematically in Figure 3.1. The output section comprises 12 cavities. The first and last two cavities are tuned to a higher frequency and are labeled type II. The eight central cavities are called type I. The Brillouin diagrams for the two objective circuit types are shown in Figure 3.2. This circuit arrangement has been found to enhance electronic stability.

The exact cavity dimensions chosen for the new circuit were slight modifications on an existing circuit. The cavity plates were made as thin as possible to optimize R/Q without being made so thin as to be thermally and mechanically unstable. The dimensions chosen for the two cavity types are shown in Table 3.1.

	TYPE I	TYPE II
Circuit Period	1.050	0.800
Cavity Height	0.950	0.700
Cavity Diameter	1.840	2.035
Tunnel Diameter	0.443	0.443
Cavity Gap	0.350	0.300
Slot Width	0.562	0.562
Slot Length	1.332	1.435

TABLE 3.1

Cavity Dimensions of Two Circuit Types in Inches

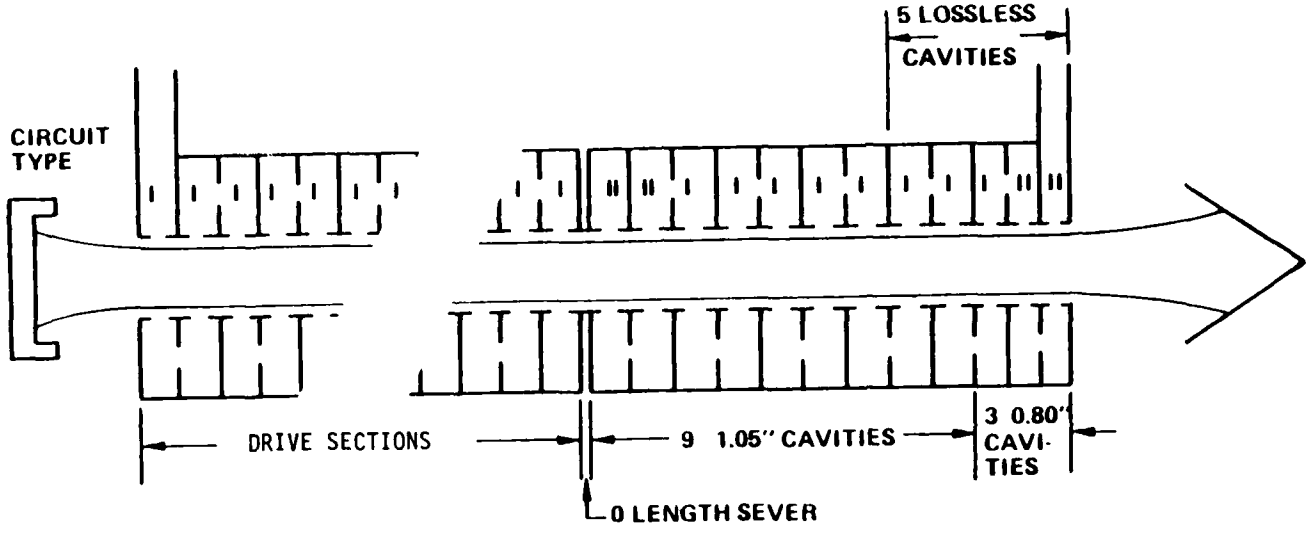

FIGURE 3.1 **SCHEMATIC FOR 100 kW S-BAND COUPLED-CAVITY TWT**

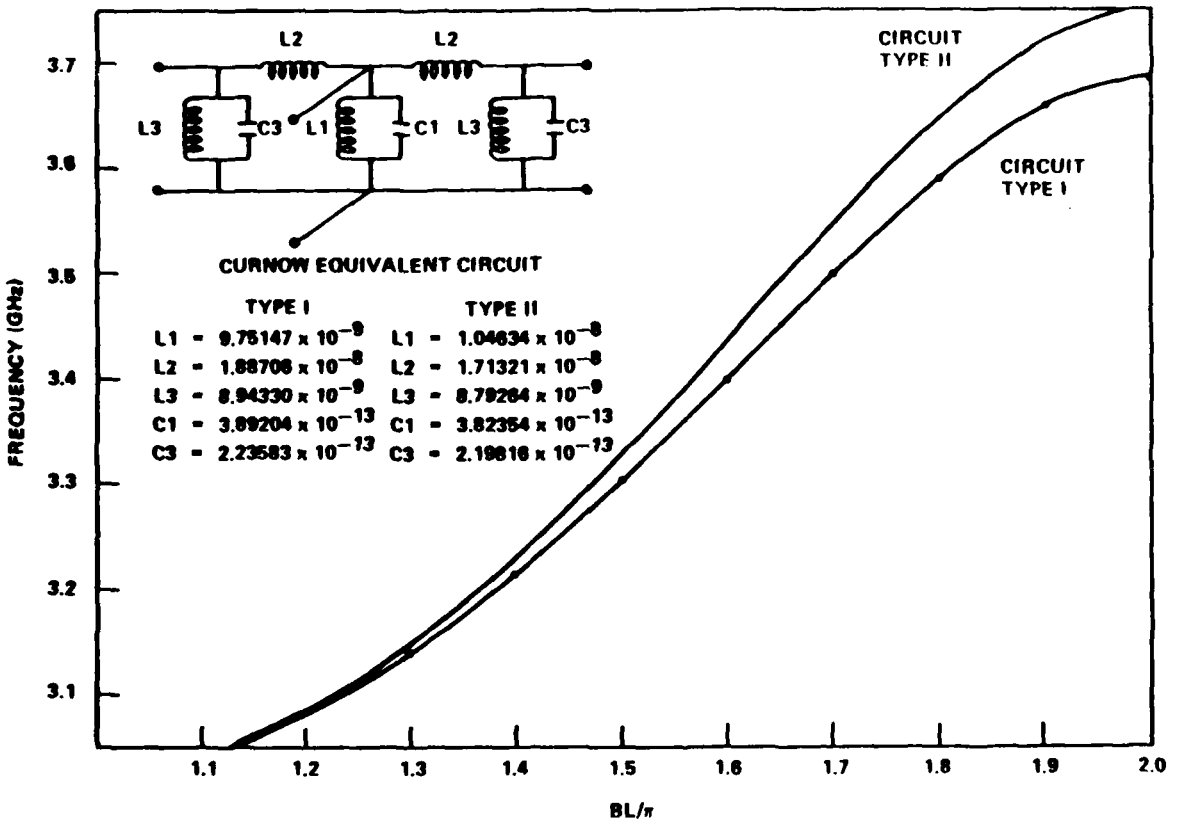

FIGURE 3.2 BRILLOUIN DIAGRAMS FOR TWO CIRCUIT TYPES EMPLOYED IN DESIGN STUDY FOR HIGH EFFICIENCY S-BAND TWT

The type II dimensions in the table are for the type II cavities at the output end of the circuit. The type II cavities at the input (sever) end are special lossy cavities which are empirically modified type I lossy cavities.

The measured Brillouin Diagram for the two circuit types is shown in Figure 3.3. The bandwidth of these two circuit types can be seen to closely match the objectives shown in Figure 3.2.

The type I circuit was found to have an R/Q of 131 by perturbation measurement. The measured R/Q for the type II circuit is 116. The measured phase and impedance data were used to derive lumped equivalent circuits which were subsequently used in conjunction with Varian computer programs to predict the performance of the TWT.

The first seven cavities of the output circuit are lossy and the last five lossless. The first iteration computation was done assuming a trial value of loss to check computationally to see if the circuit section would be electronically stable. The object of this procedure was to find the minimum loss which will yield stable operation. As a result of these computations, a Q of 18 was chosen for the lossy cavities. The predicted start oscillation current for a circuit with this loss is shown in Figure 3.4. Since the nominal beam current is 8A and the nominal beam voltage is 41 KV, this figure shows a stability margin of over 40 percent. This design was chosen even though a lesser margin may have been feasible. It is always possible to run a TWT at higher beam currents to check for efficiency up to the beam current where instability sets in.

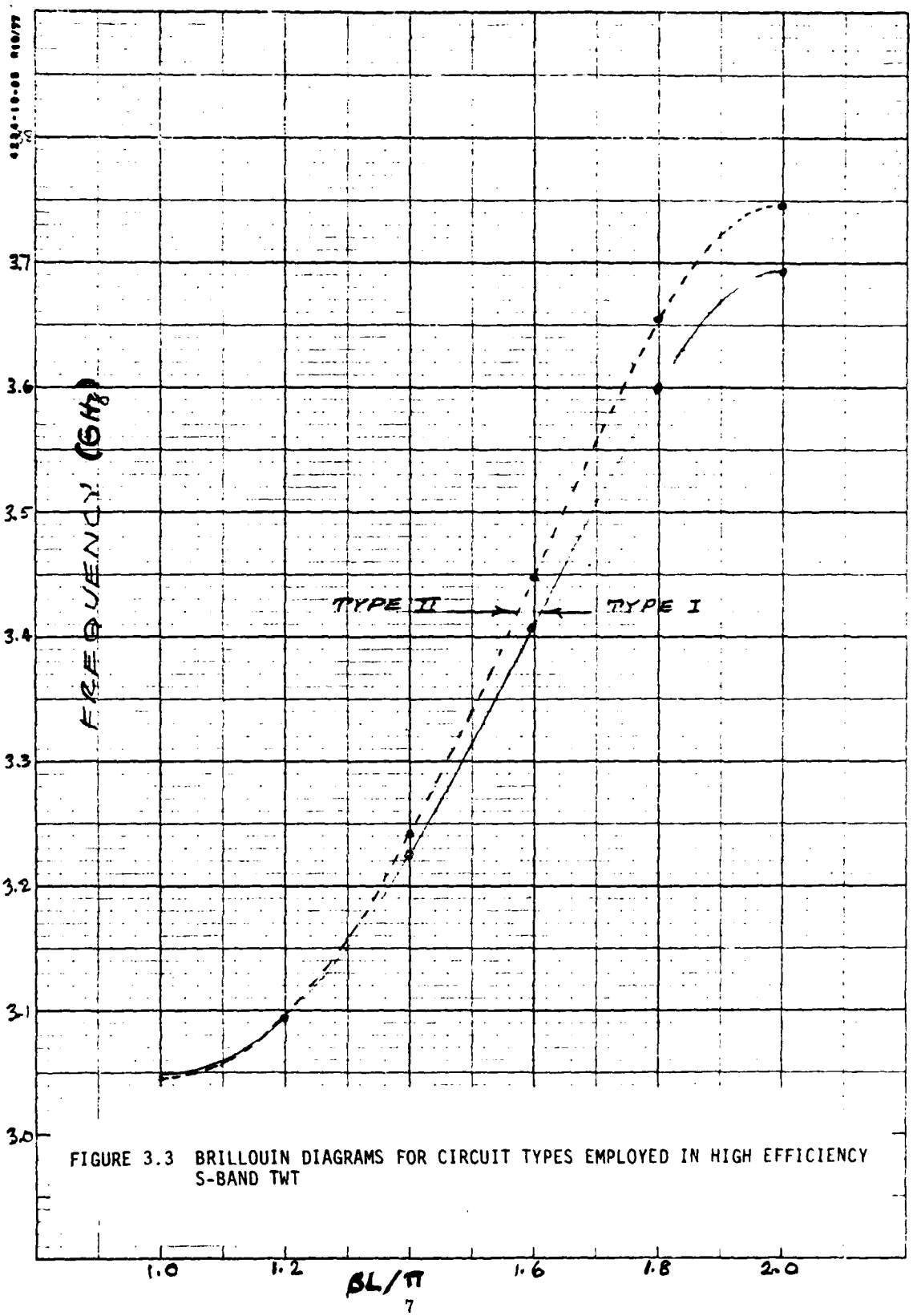

FIGURE 3.3 BRILLOUIN DIAGRAMS FOR CIRCUIT TYPES EMPLOYED IN HIGH EFFICIENCY S-BAND TWT

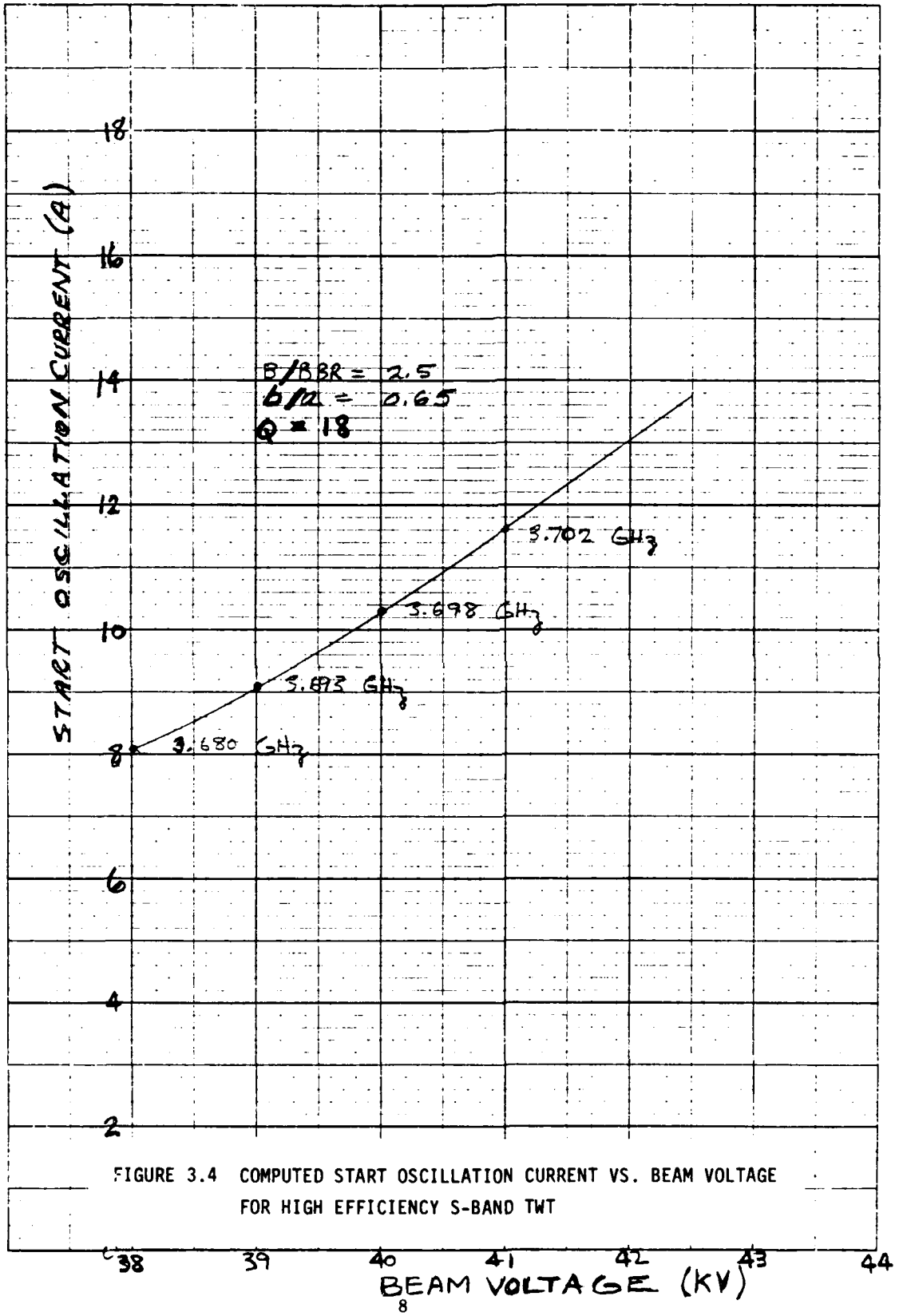

FIGURE 3.4 COMPUTED START OSCILLATION CURRENT VS. BEAM VOLTAGE FOR HIGH EFFICIENCY S-BAND TWT

The required circuit loss was obtained by setting lossy ceramic cylinders into the walls of the cavities as shown in Figure 3.5. Because these cylinders of lossy ceramic contact the copper body over most of their surface area, they are thermally rugged and stable. The measured insertion loss for the output circuit is shown in Figure 3.6. This measurement is taken using a specially matched coupling cavity in place of the sever cavity.

The output match employs a double tapered waveguide, similar to that employed on the VTS-5753. The measured match looking into the output waveguide is shown in Figure 3.7. The match is excellent over a full 500 MHz.

The sever load is similar to that used in the VTS-5753. It employs three blocks of lossy ceramic empirically tuned to provide an excellent match.

3.3 Overall TWT

The gun employed in the first prototype tube is the same gun used in the VTS-5753. This gun was chosen because the originally planned Brillouin field gun was not developed in time to be used in these experiments. It was intended to operate this gun, nominally used at 2.5 times Brillouin, at the lowest feasible focusing field. The focusing solenoid of the VTS-5753 was used for these tests. The input and center sections of the tube are eight and seven cavities long respectively. These circuits were taken from the VTS-5754 and have a passband which is virutally identical to the type I circuit. The collector and output window are the same ones used in the VTS-5753.

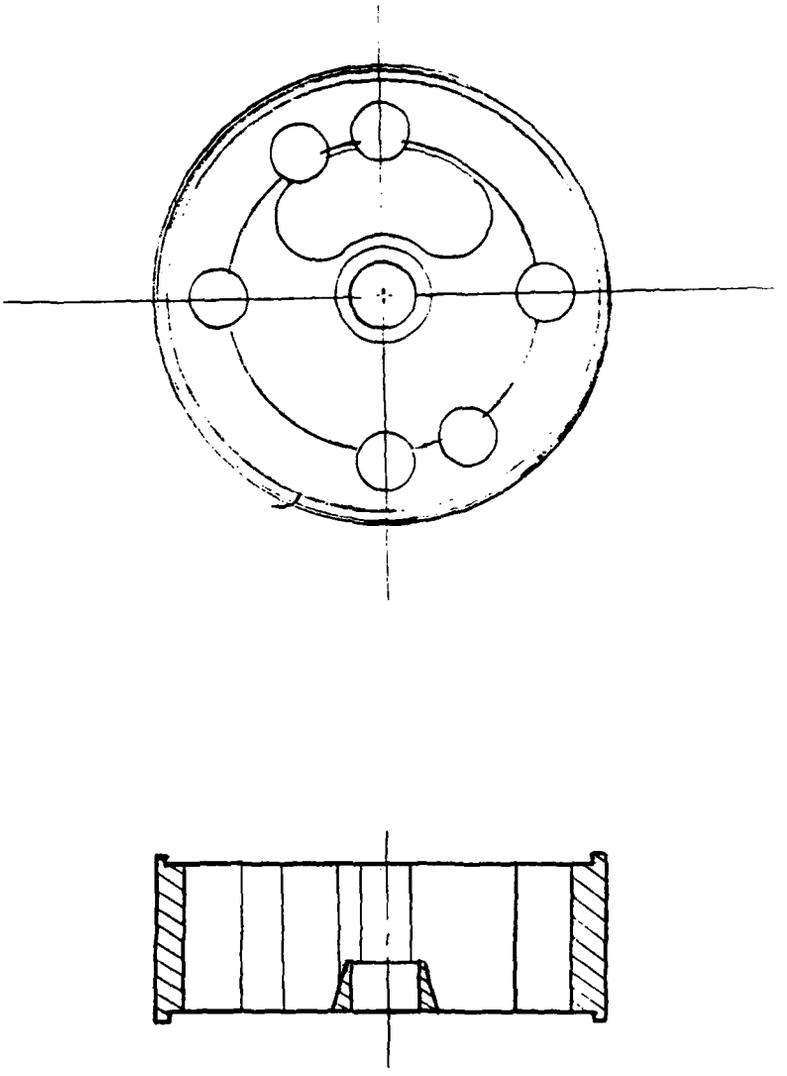

FIGURE 3.5 SKETCH SHOWING TYPE I CAVITY SPACER AND PLATE WITH LOSSY CERAMIC CYLINDERS IN CAVITY WALL

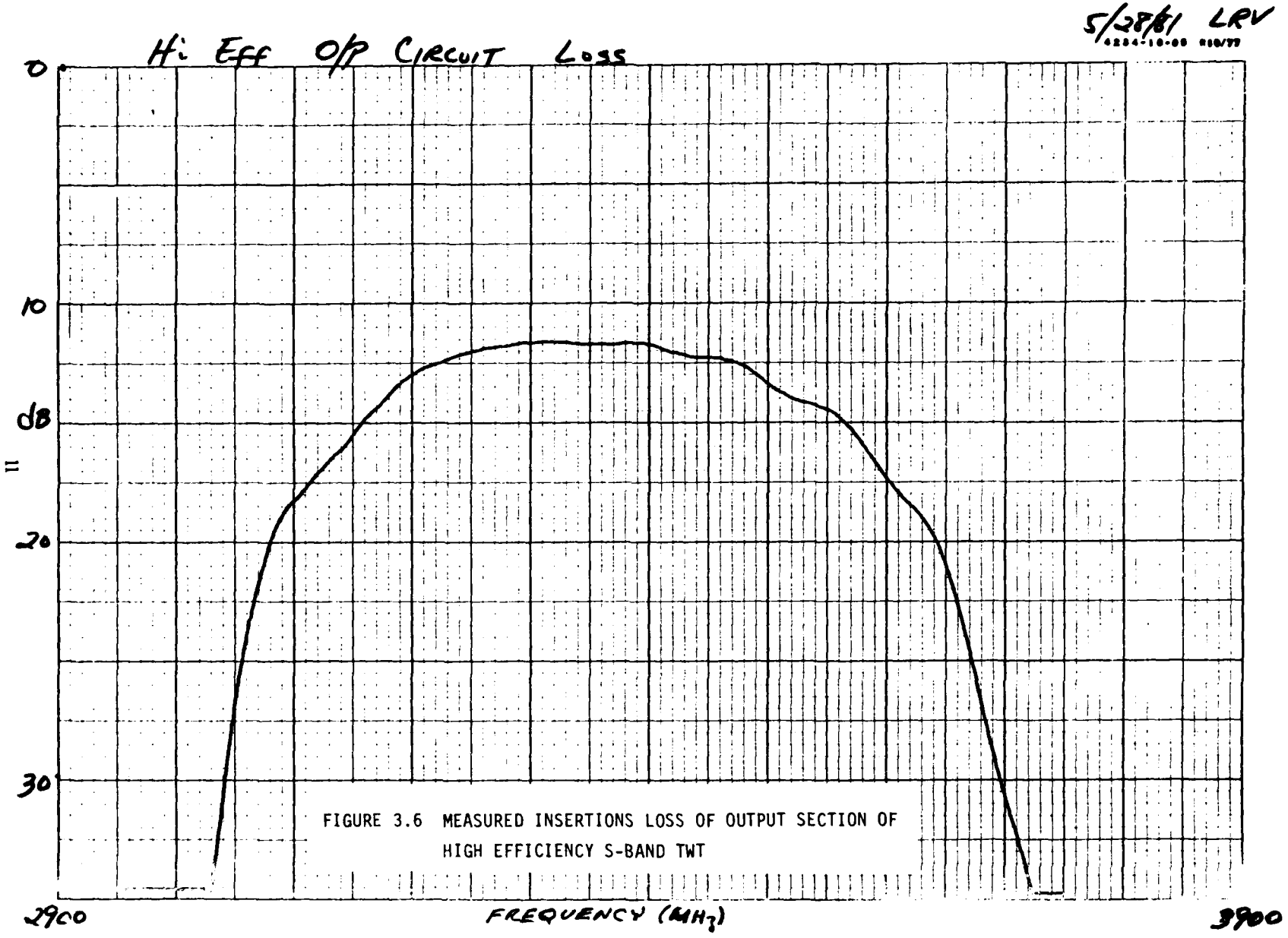

FIGURE 3.6 MEASURED INSERTIONS LOSS OF OUTPUT SECTION OF HIGH EFFICIENCY S-BAND TWT

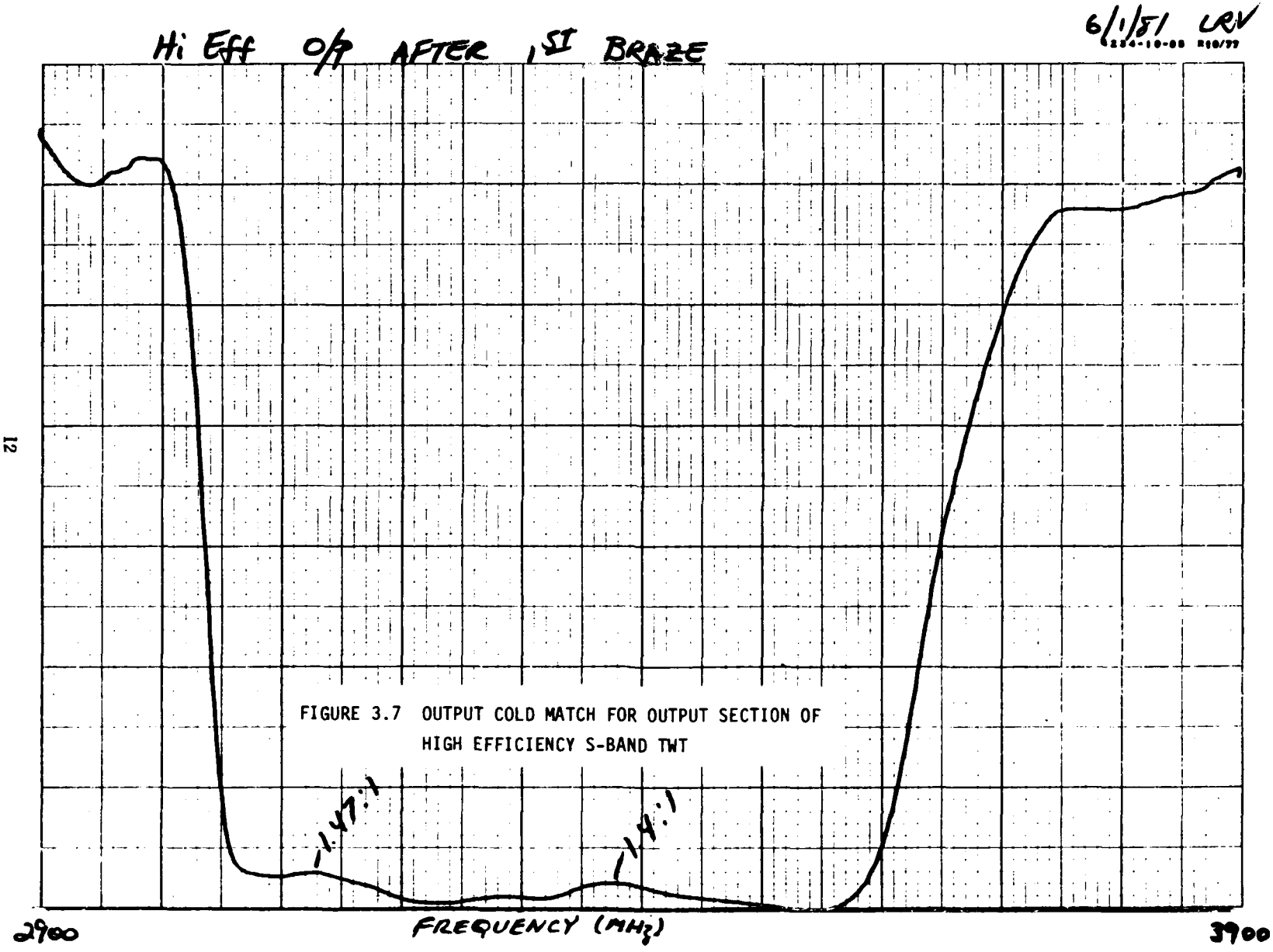

FIGURE 3.7 OUTPUT COLD MATCH FOR OUTPUT SECTION OF HIGH EFFICIENCY S-BAND TWT

3.4 Predicted Performance

Computer analysis was carried out using the measured circuit characteristics and assuming a beam current of 9 A and a beam voltage of 42 KV with a filling factor of 0.65 and a magnetic field 2.5 times the Brillouin Field. The predicted small signal gain is shown in Figure 3.8. The gain exceeds the specified 40 dB over the required 500 MHz bandwidth.

The large signal predicted performance is shown in Figure 3.9. The predicted efficiency is below specification. Further trimming of the beam voltage beam current and beam diameter can be expected to improve the efficiency as is demonstrated in Section 4.

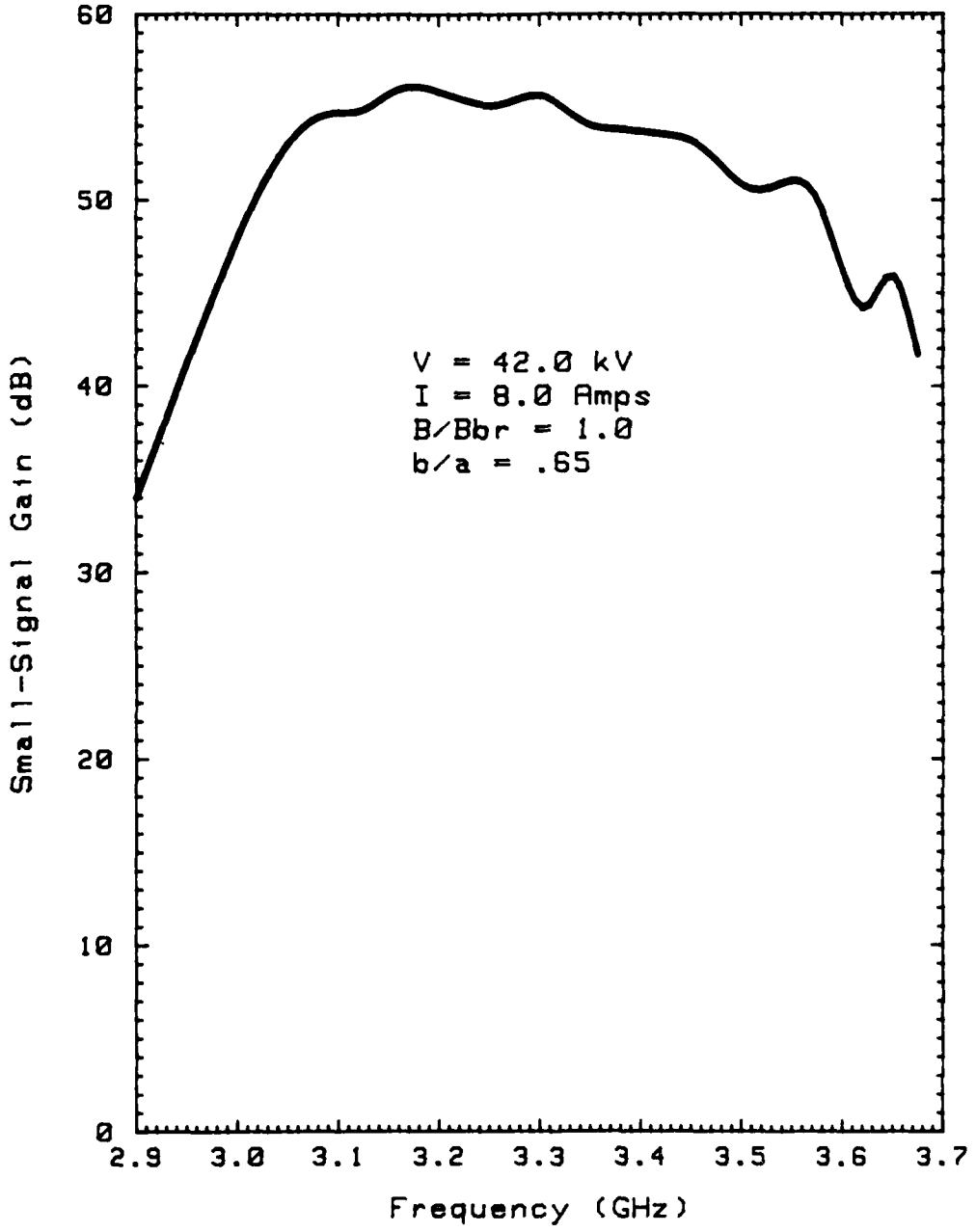

FIGURE 3.8 PREDICTED SMALL SIGNAL GAIN FOR HIGH EFFICIENCY S-BAND TWT

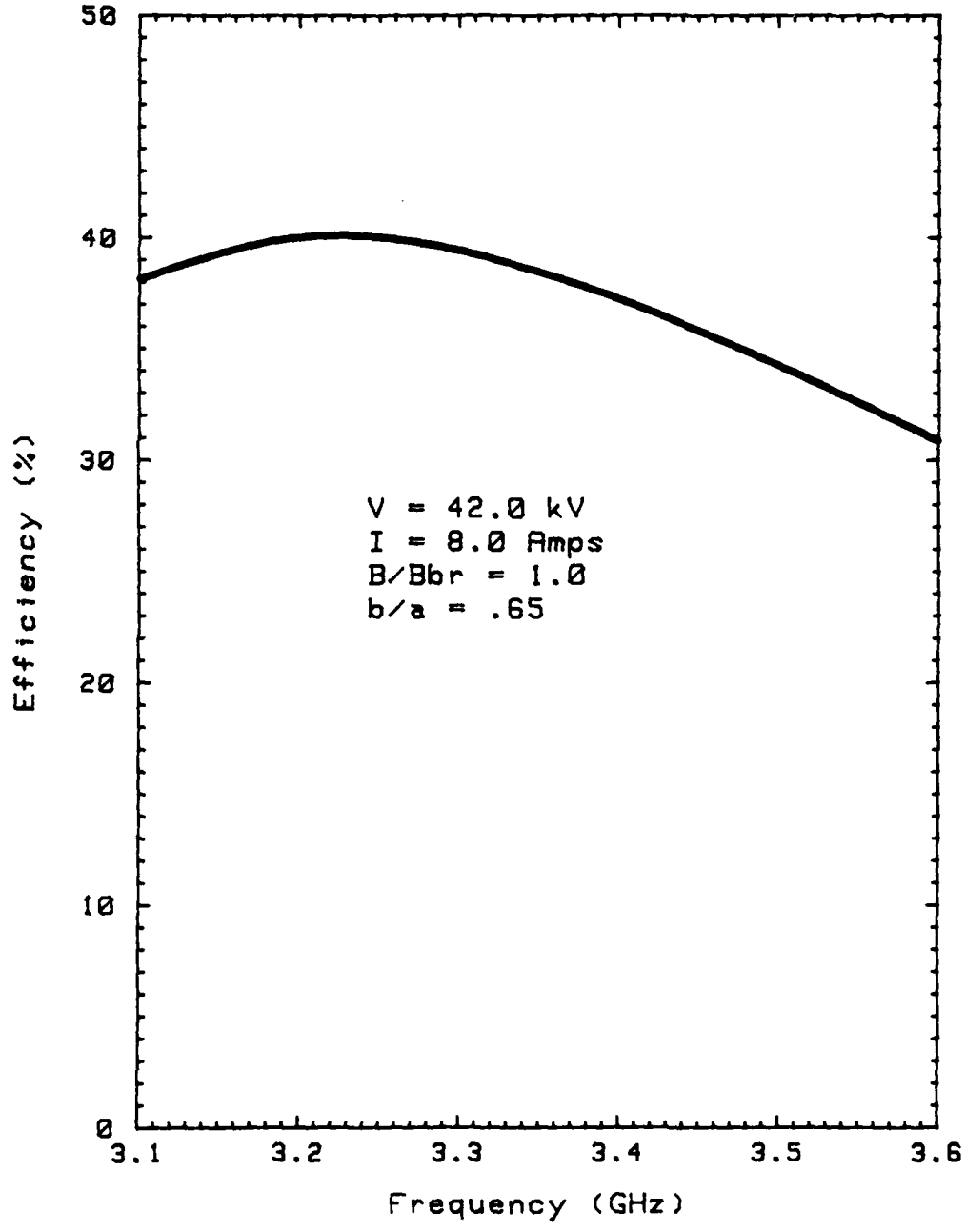

FIGURE 3.9 PREDICTED CONVERSION EFFICIENCY FOR HIGH EFFICIENCY S-BAND TWT

4.0 EXPERIMENTAL TEST OF TWT

4.1 Introduction

Hot testing of this TWT was carried out without incident. There were no leaks and there was insignificant arcing. The tube was run for approximately 100 hours at a duty factor of 0.001. The duty factor was then increased up to 0.10 for a maximum average power greater than 13 KW.

Testing was carried out over a range of magnetic focusing fields using a gun coil to attempt to maintain good focusing. It was found impossible to reduce the magnet field below 2.5 B_{br} without high beam interception.

4.2 Test Results

Figures 4.1 through 4.3 show power output vs. frequency with drive power as a parameter. At 41 KV and 8 A (Figure 4.1) the tube exhibits reasonably flat gain over the design band, 3.1 to 3.6 GHz. The upper curve represents the drive power required to saturate at 3.1 GHz. The relative power output at the bottom of the band is somewhat low , perhaps a result of excessive circuit loss chosen to ensure electronic stability.

At 42 KV and 8 A (Figure 4.2) the power output at 11.5 W drive is somewhat flatter and slightly increased. The small signal gain shows a normal downward ramp which is typical for tubes of this type run at a voltage which gives the flattest saturated power output. The slight power notch at the lower band edge persists.

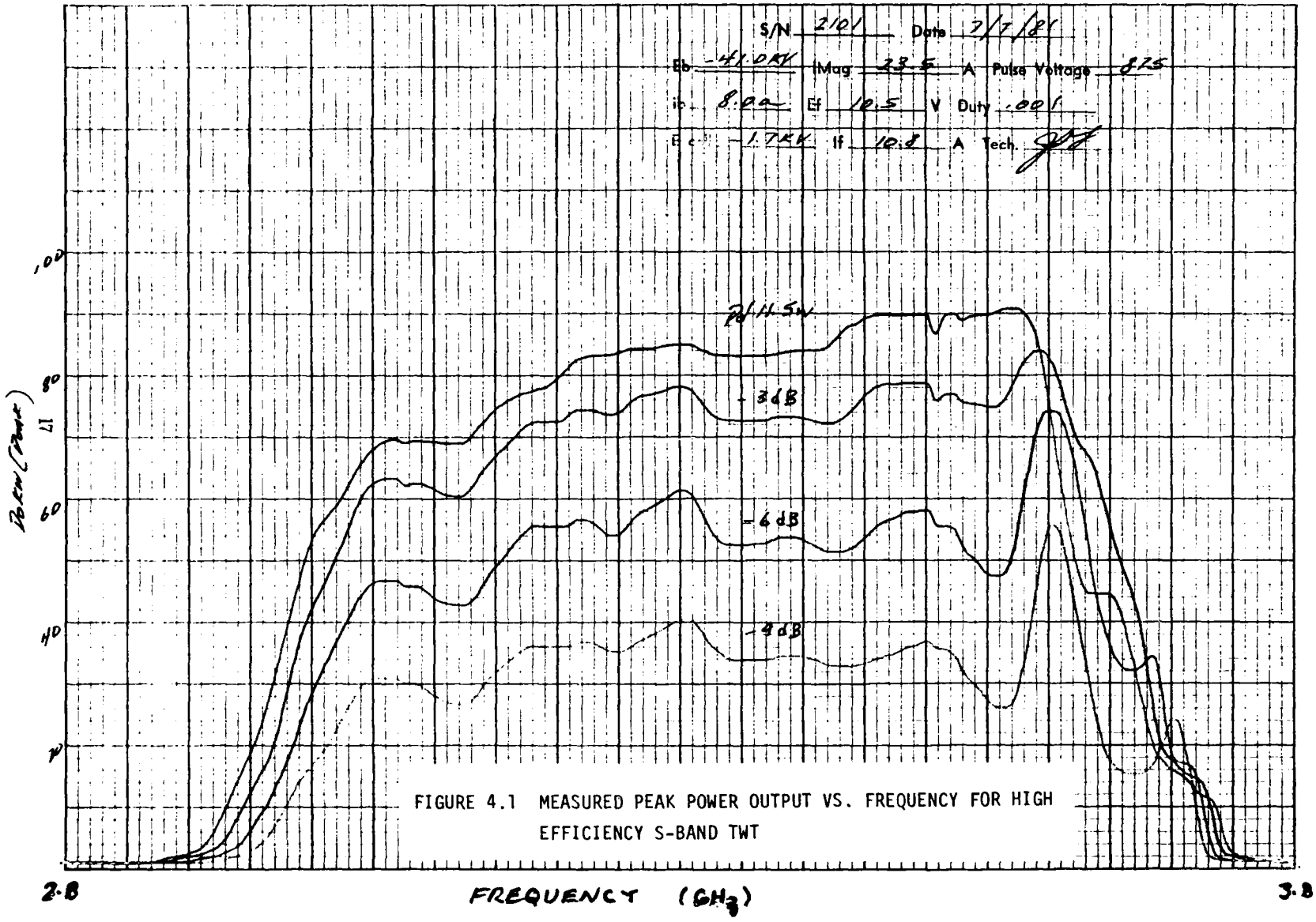

FIGURE 4.1 MEASURED PEAK POWER OUTPUT VS. FREQUENCY FOR HIGH EFFICIENCY S-BAND TWT

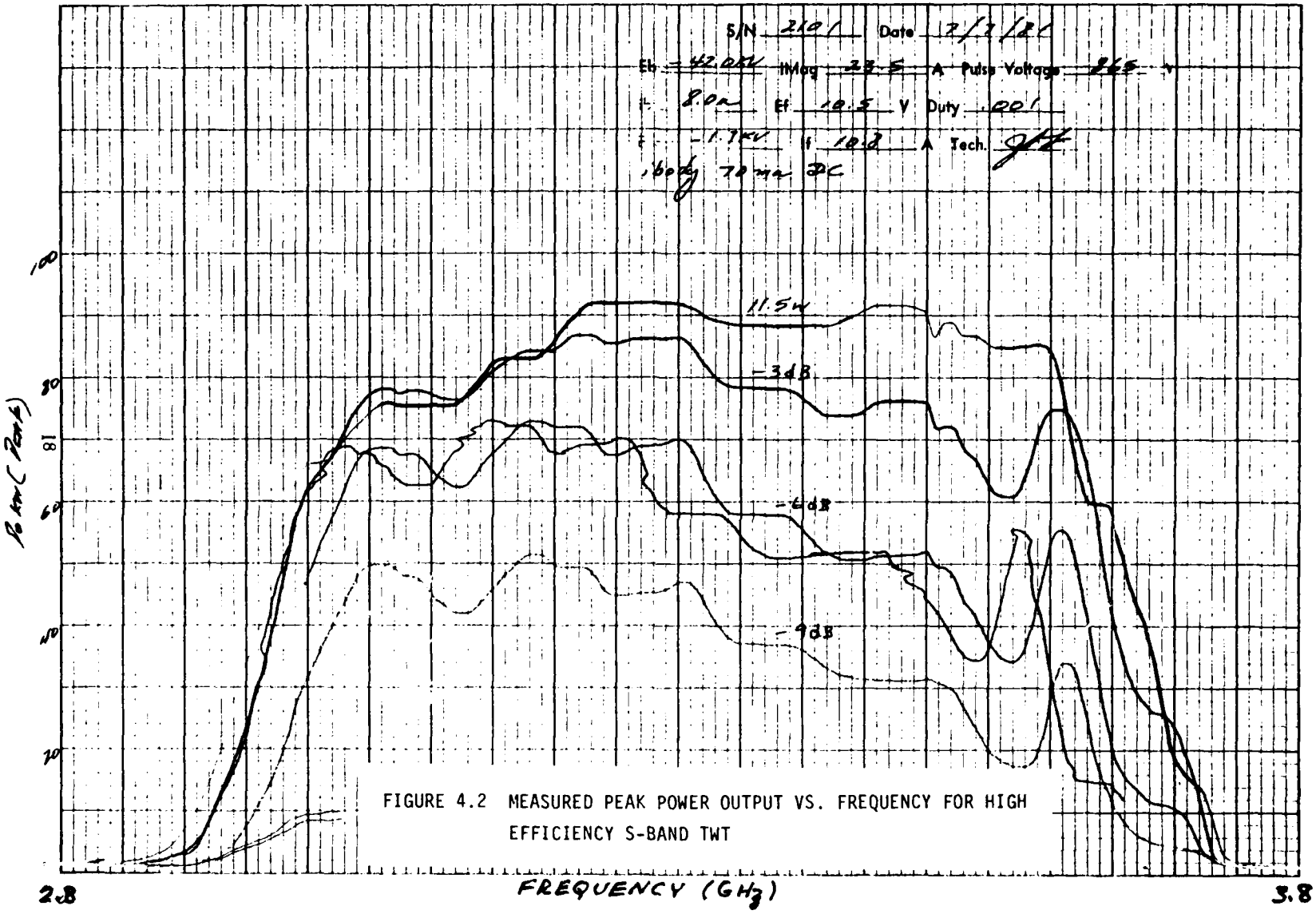

FIGURE 4.2 MEASURED PEAK POWER OUTPUT VS. FREQUENCY FOR HIGH EFFICIENCY S-BAND TWT

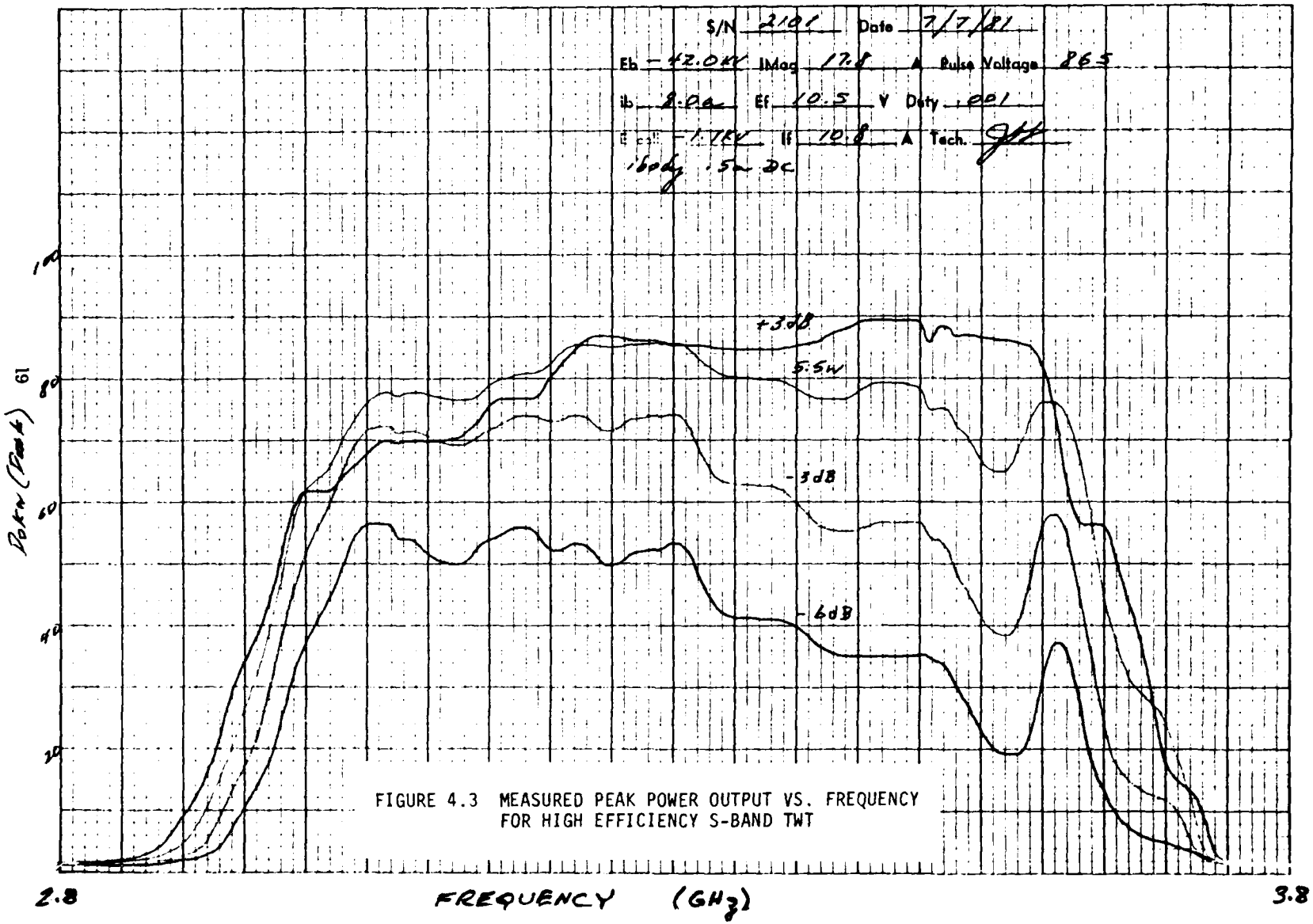

FIGURE 4.3 MEASURED PEAK POWER OUTPUT VS. FREQUENCY FOR HIGH EFFICIENCY S-BAND TWT

Figure 4.3 shows the effect of reducing the focusing field by 25 percent. The DC body current has increased from 70 ma to 500 ma. The saturated power is slightly less than before, whereas the small signal gain at the bottom of the band has increased.

Figure 4.4 shows the output hot match. This match is completely acceptable. At 42 KV the tube might become unstable at the upper band edge if operated into a 100 percent reflecting load.

The input hot match is shown in Figure 4.5. This excellent hot match is, in part, the result of using a relatively short input circuit.

Figures 4.6 through 4.10 show the output power vs frequency with drive power as a parameter. In each case, the drive power required to saturate at 3.1 GHz is defined at 0 dB. Figures 4.6 through 4.8 show the effect of charging the magnetic focusing field. With the lowest focusing field (Solenoid current = 14.5 A) the body current is excessive and the gain and power output is low. At 18.9 A solenoid current, the performance is optimum using a 10 wrap gun coil running at 15 A. The saturated power at 3.5 GHz is greater than 100 KW.

Figure 4.8 shows a slightly different focusing field and gun coil. The performance is slightly degraded relative to the previous figure.

Figure 4.9 shows the consequence of increasing the beam current from 8 A to 9 A. The output power has increased by a little more than the beam power and the gain has increased by approximately 2 dB. The saturated peak power is more than 100 KW.

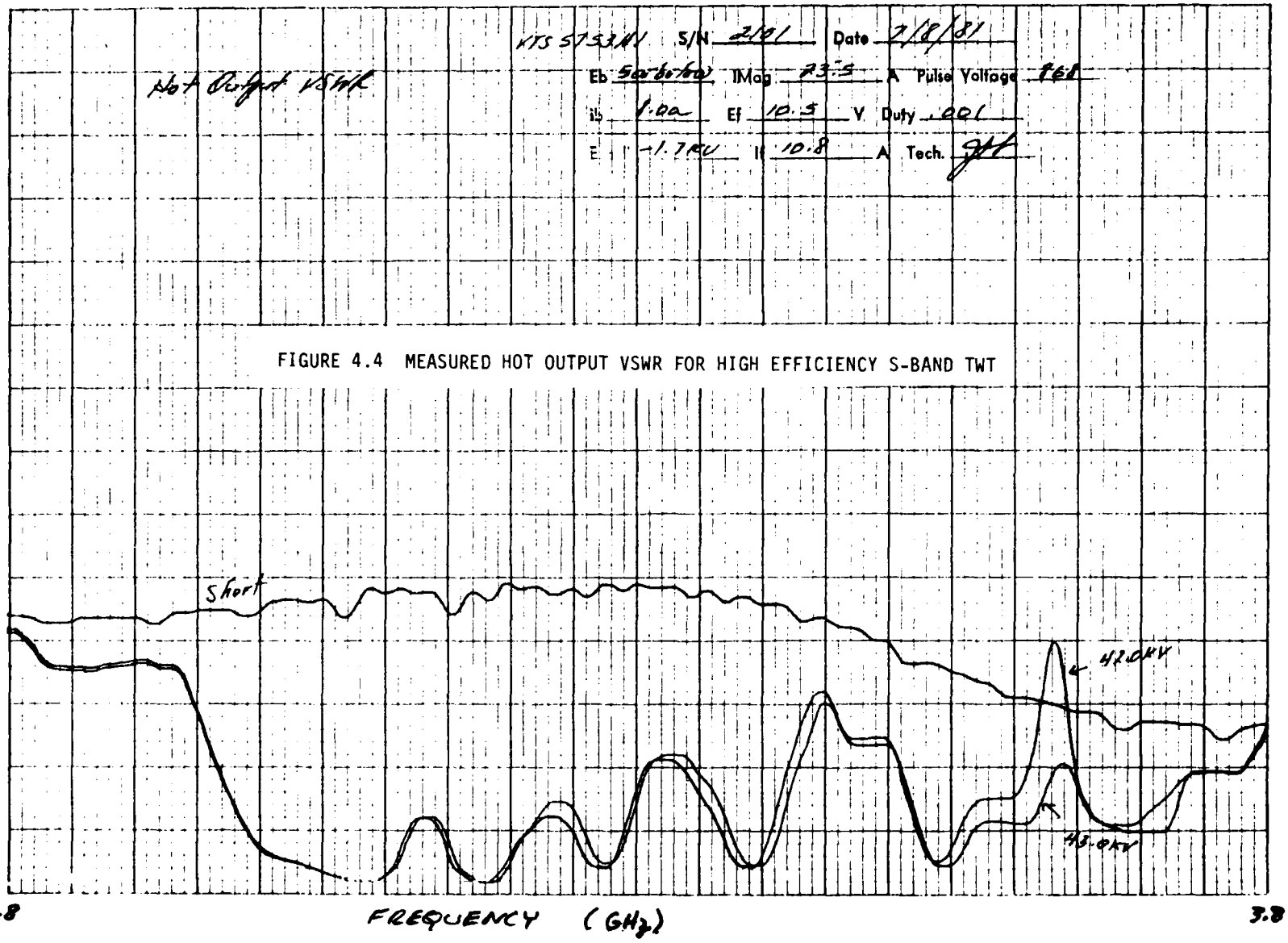

FIGURE 4.4 MEASURED HOT OUTPUT VSWR FOR HIGH EFFICIENCY S-BAND TWT

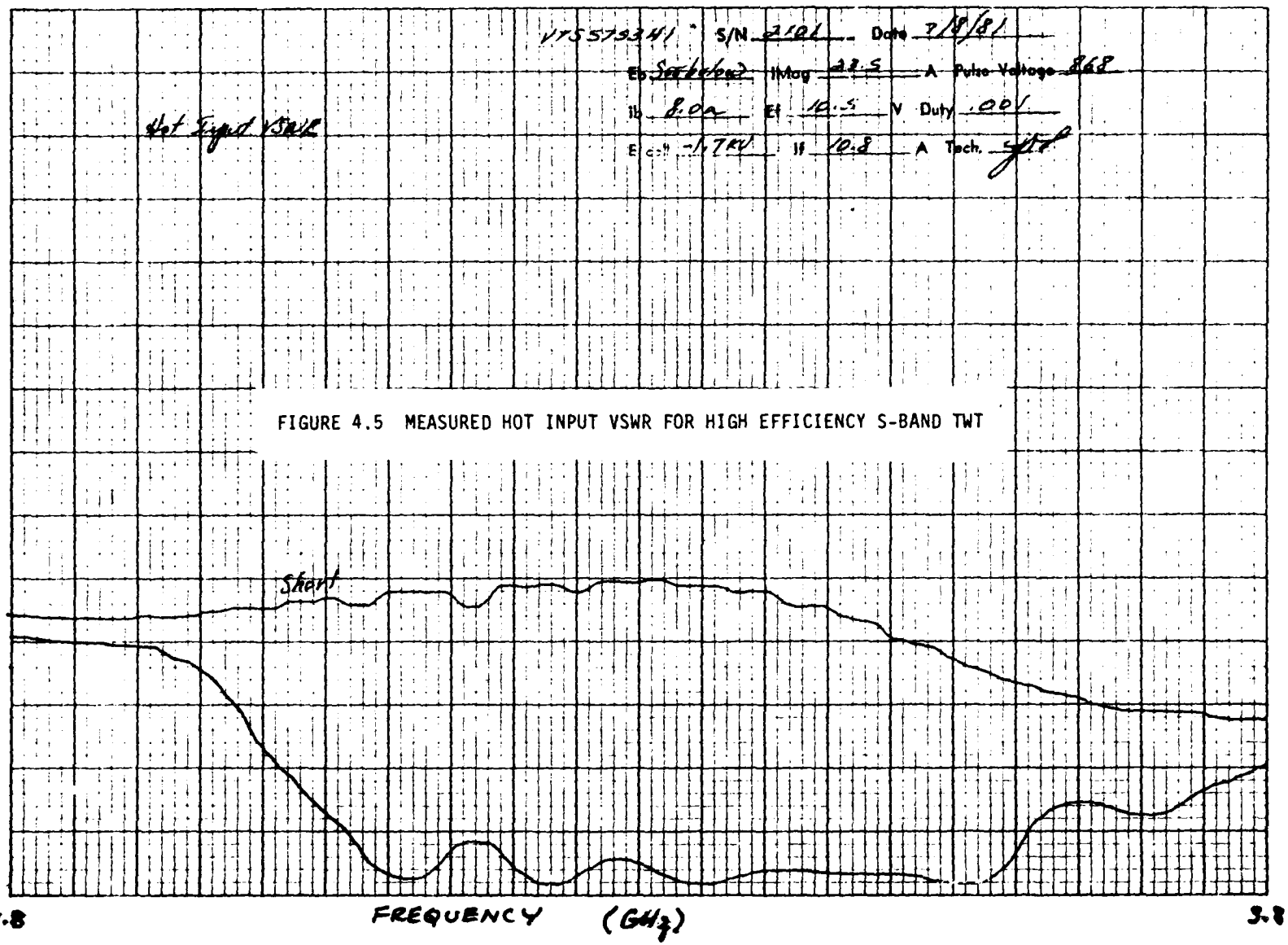

FIGURE 4.5 MEASURED HOT INPUT VSWR FOR HIGH EFFICIENCY S-BAND TWT

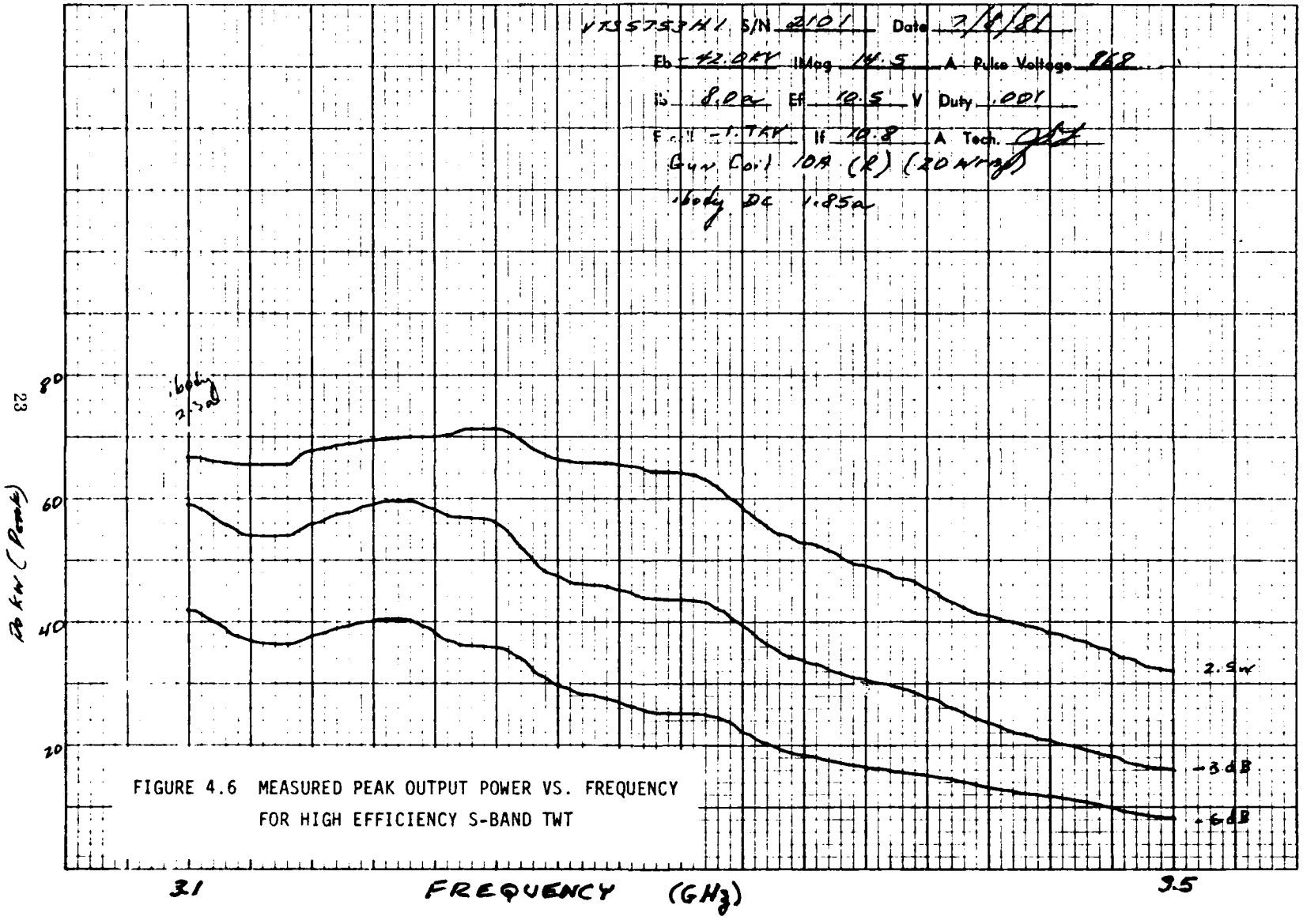

FIGURE 4.6 MEASURED PEAK OUTPUT POWER VS. FREQUENCY FOR HIGH EFFICIENCY S-BAND TWT

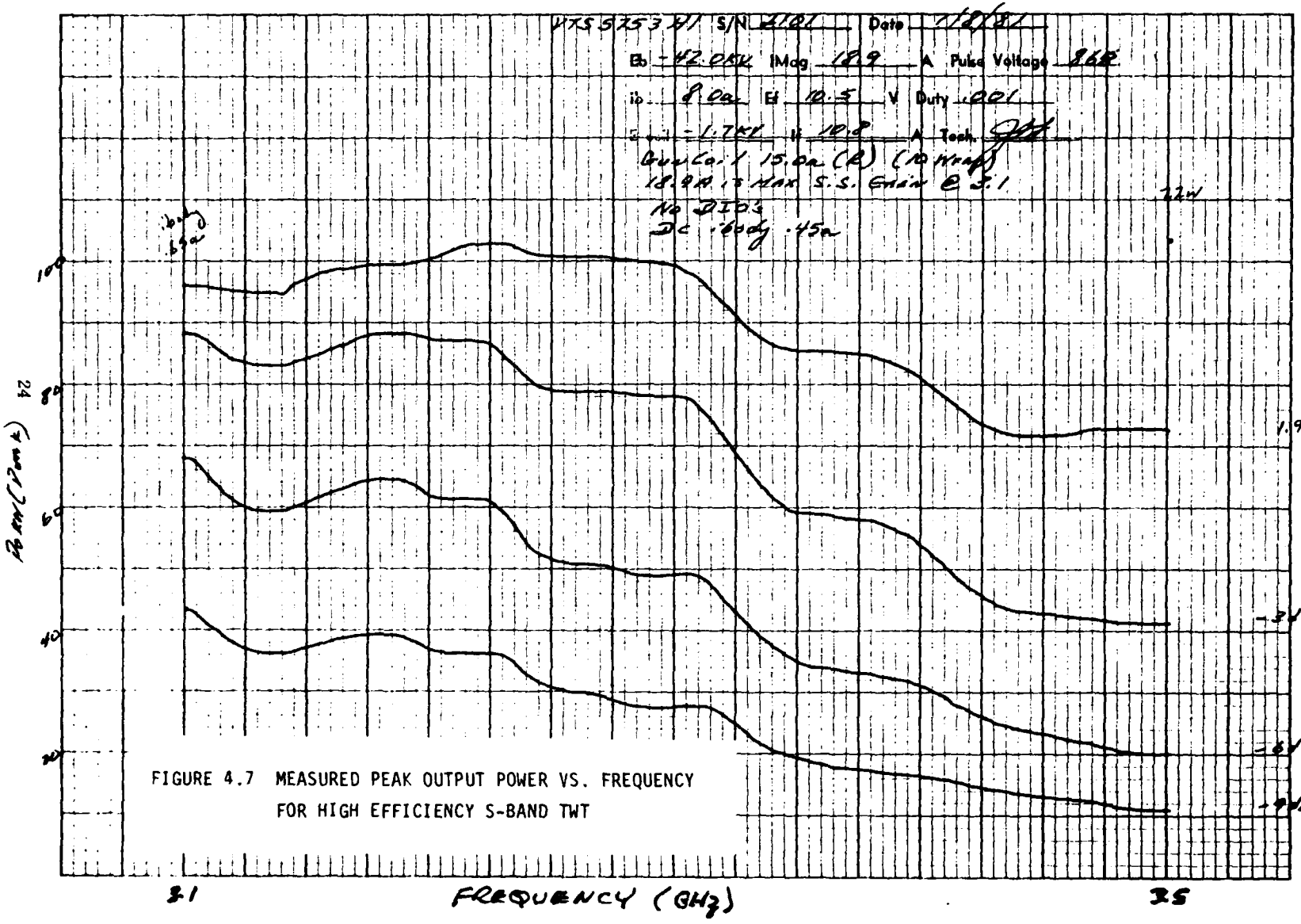

FIGURE 4.7 MEASURED PEAK OUTPUT POWER VS. FREQUENCY FOR HIGH EFFICIENCY S-BAND TWT

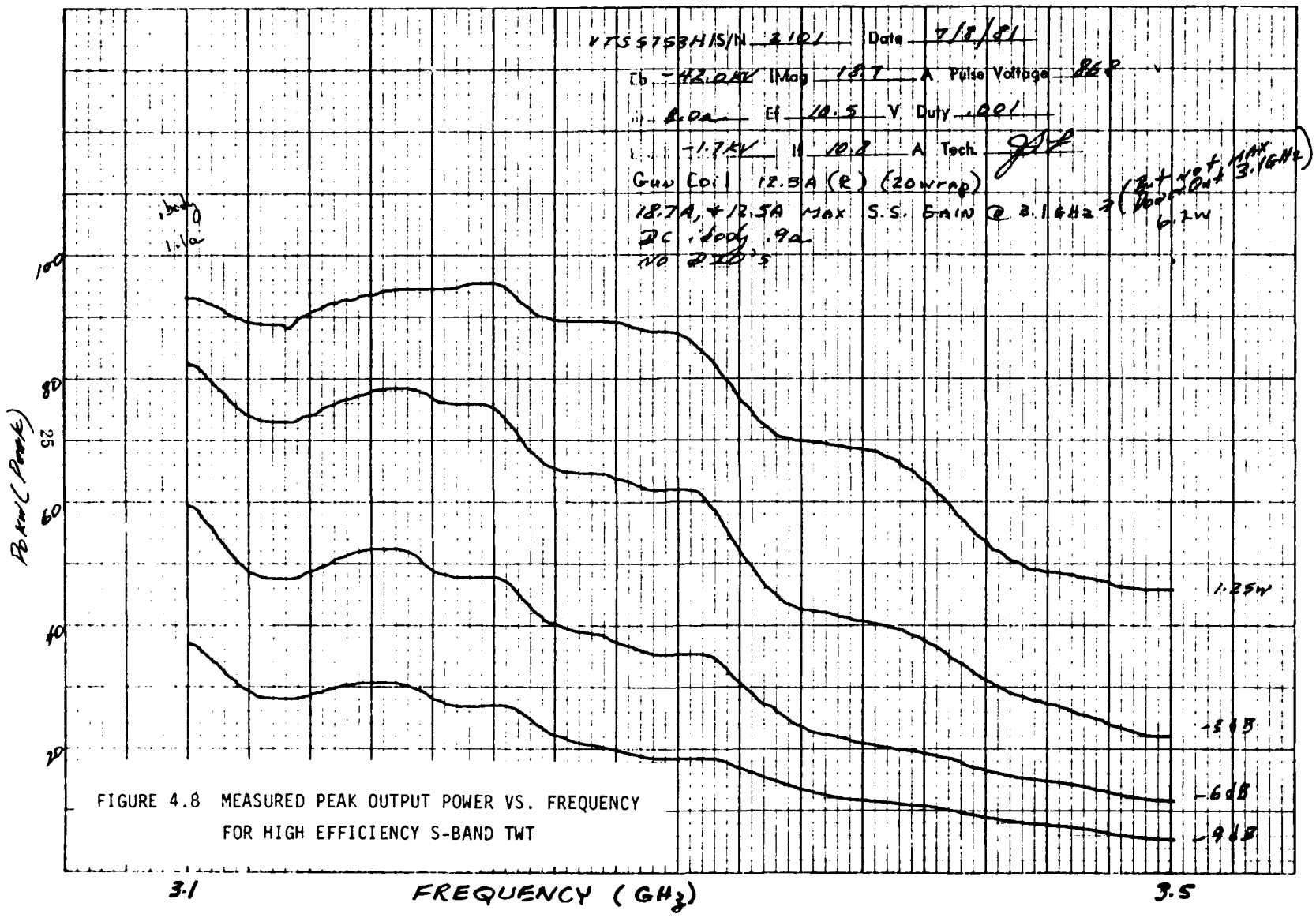

FIGURE 4.8 MEASURED PEAK OUTPUT POWER VS. FREQUENCY FOR HIGH EFFICIENCY S-BAND TWT

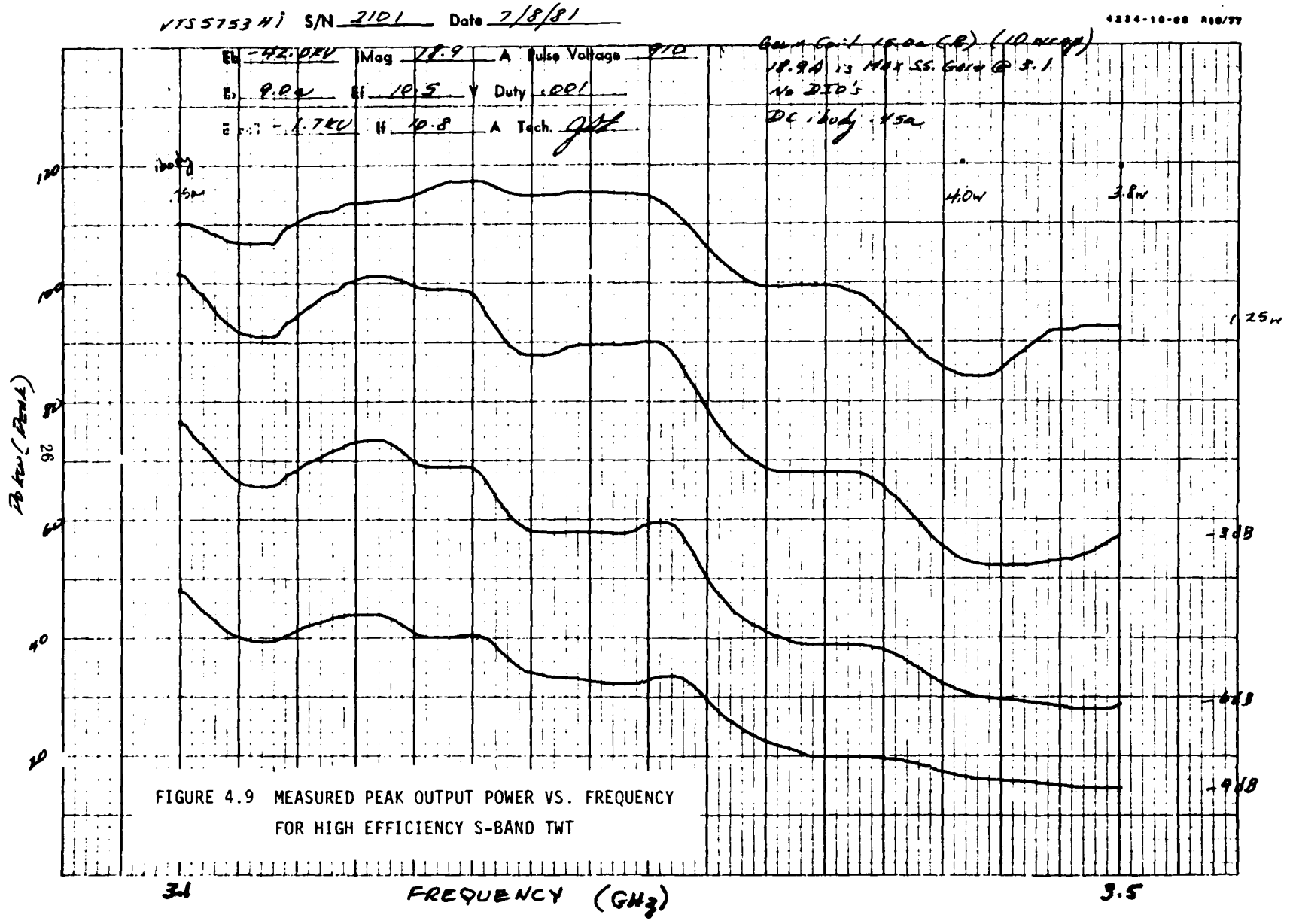

FIGURE 4.9 MEASURED PEAK OUTPUT POWER VS. FREQUENCY FOR HIGH EFFICIENCY S-BAND TWT

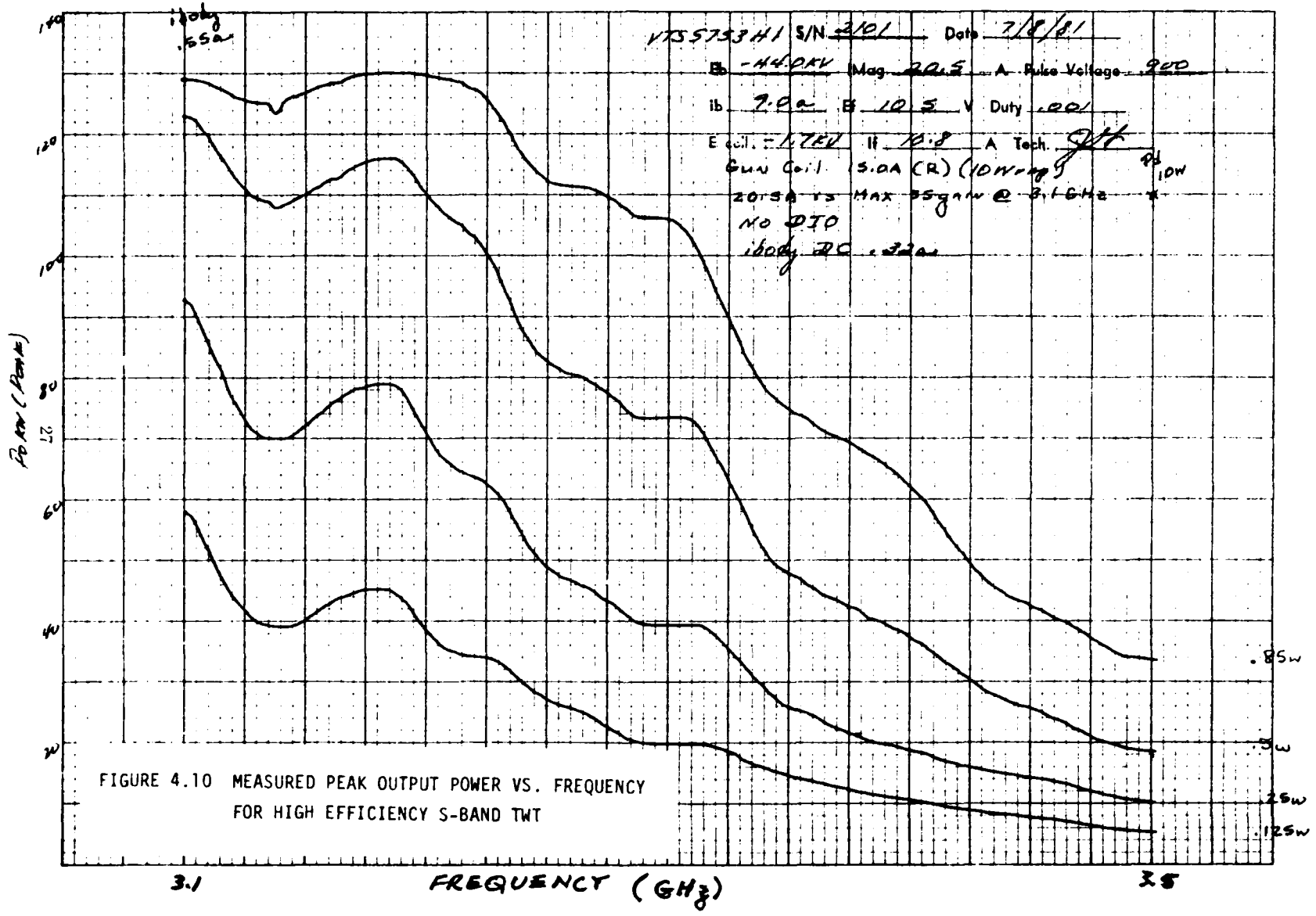

FIGURE 4.10 MEASURED PEAK OUTPUT POWER VS. FREQUENCY FOR HIGH EFFICIENCY S-BAND TWT

Figure 4.10 shows that by increasing the beam voltage to 44 KV the gain at the bottom of the band is substantially increased. There was insufficient drive to saturate the tube over most of the band. The output power reached 130 KW.

Figure 4.11 shows saturated power out vs. frequency over a 500 MHz band from 3.050 GHz to 3.550 GHz. The saturated output is greater than 100 KW and flat to within 0.5 dB.

Figure 4.12 is similar to Figure 4.9 except that the focusing field has been increased to reduce beam interception. The power is greater than 100 KW over the frequency range 3.1 to 3.5 GHz with a fixed drive of approximately 2 W.

Figures 4.13 and 4.14 show the sensitivity of performance to magnetic focusing field. Figure 4.13 shows power vs. frequency using the focusing field normally employed to focus S-Band TWTs running at 16 A beam current. In Figure 4.14 a gun coil has been added and the focusing field has been adjusted for maximum power at 3.1 GHz. This change in focusing has increased the efficiency by almost 1 dB.

Figures 4.15 and 4.16 show measured output power and efficiency near band center. Figure 4.15 shows the power output and efficiency from 3.2 to 3.3 GHz with a 9 A beam for three values of beam voltage. At 42.5 KV the efficiency exceeds 32 percent. Figure 4.15 shows the improvement in conversion efficiency available by depressing the collector. The collector employed is a simple isolated collector without multiple stages and with no attempt to optimize it for depressed collector operation. The resulting measured efficiency is as high as 44.8 percent.

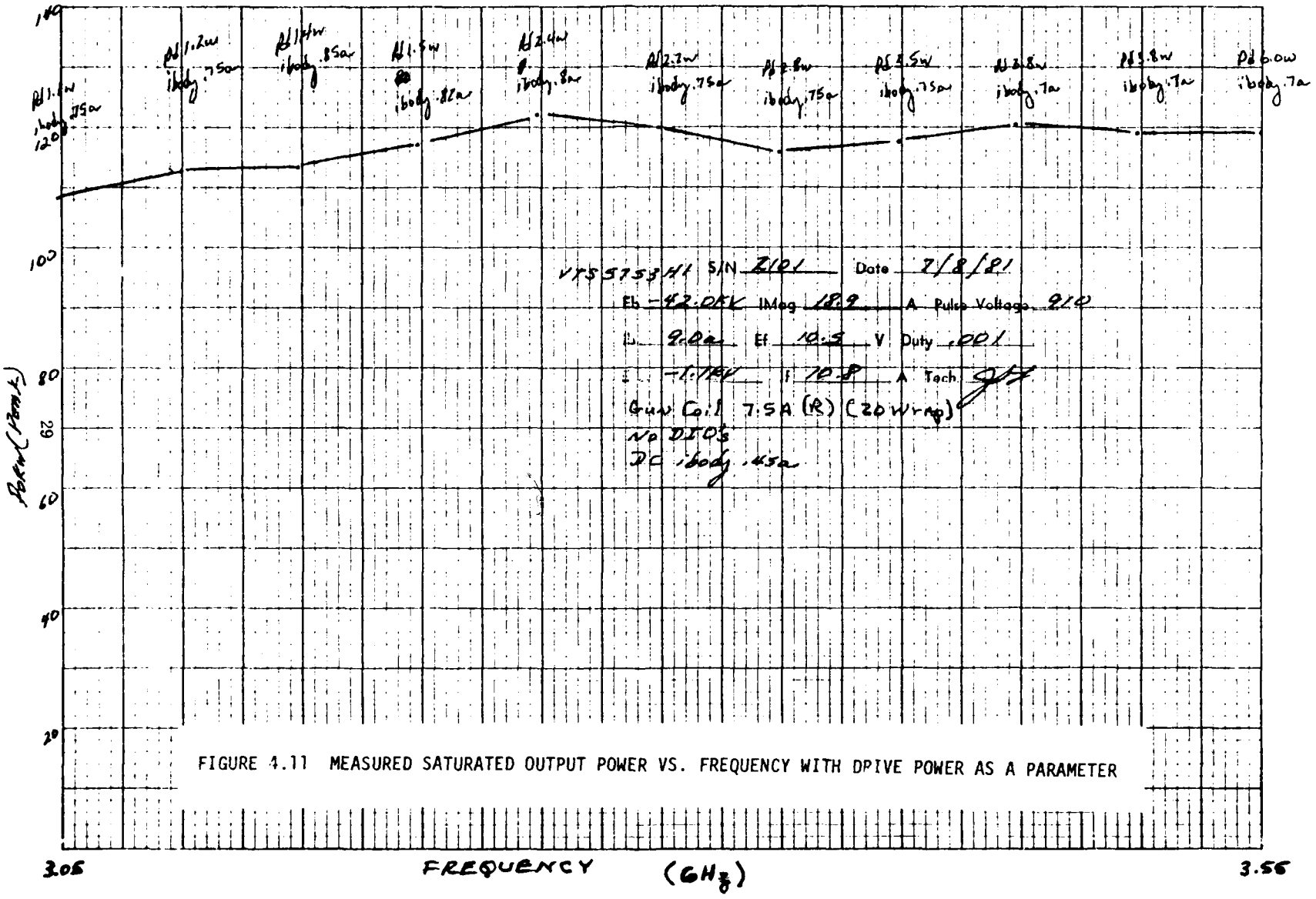

FIGURE 4.11 MEASURED SATURATED OUTPUT POWER VS. FREQUENCY WITH DRIVE POWER AS A PARAMETER

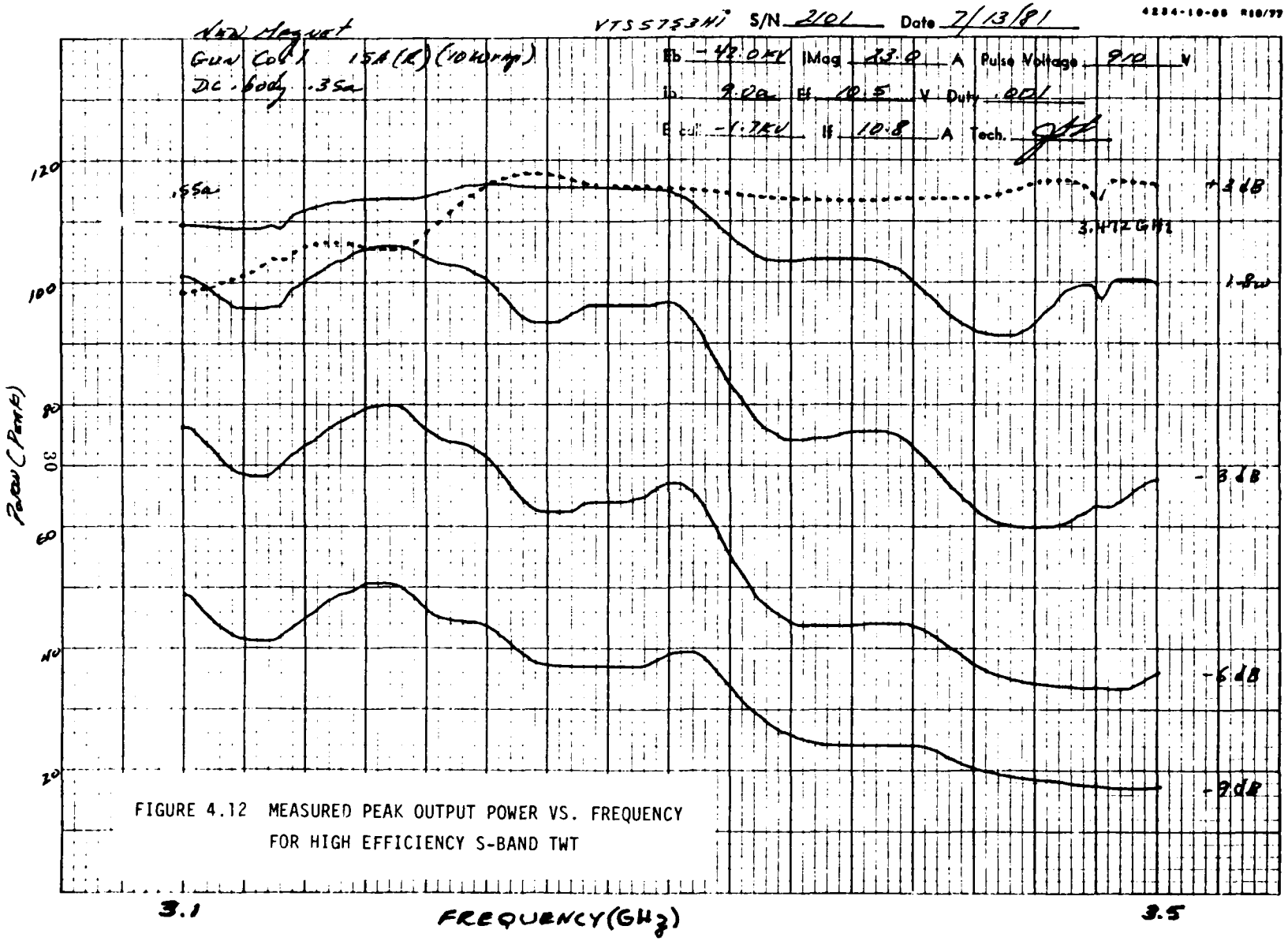

FIGURE 4.12 MEASURED PEAK OUTPUT POWER VS. FREQUENCY FOR HIGH EFFICIENCY S-BAND TWT

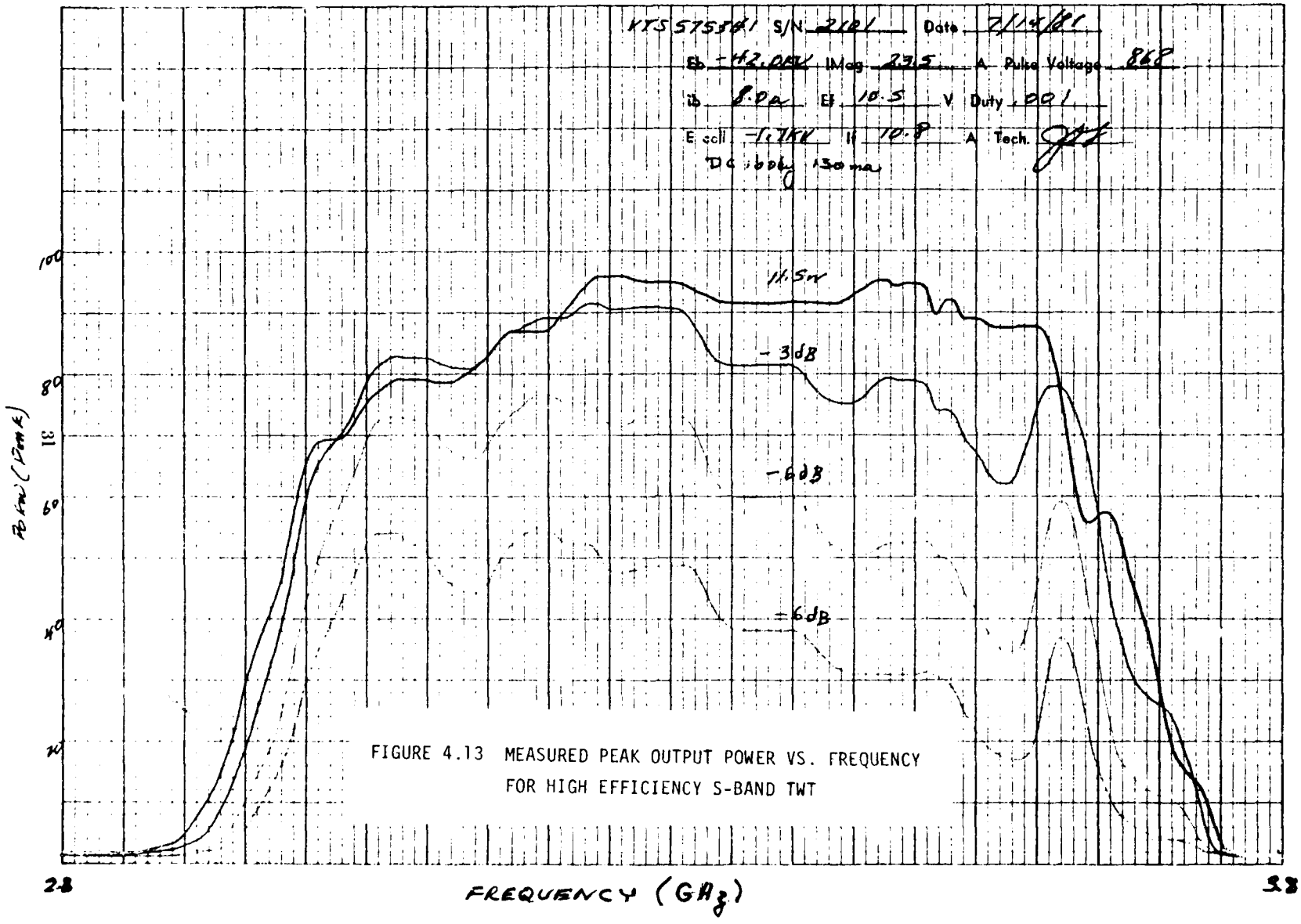

FIGURE 4.13 MEASURED PEAK OUTPUT POWER VS. FREQUENCY FOR HIGH EFFICIENCY S-BAND TWT

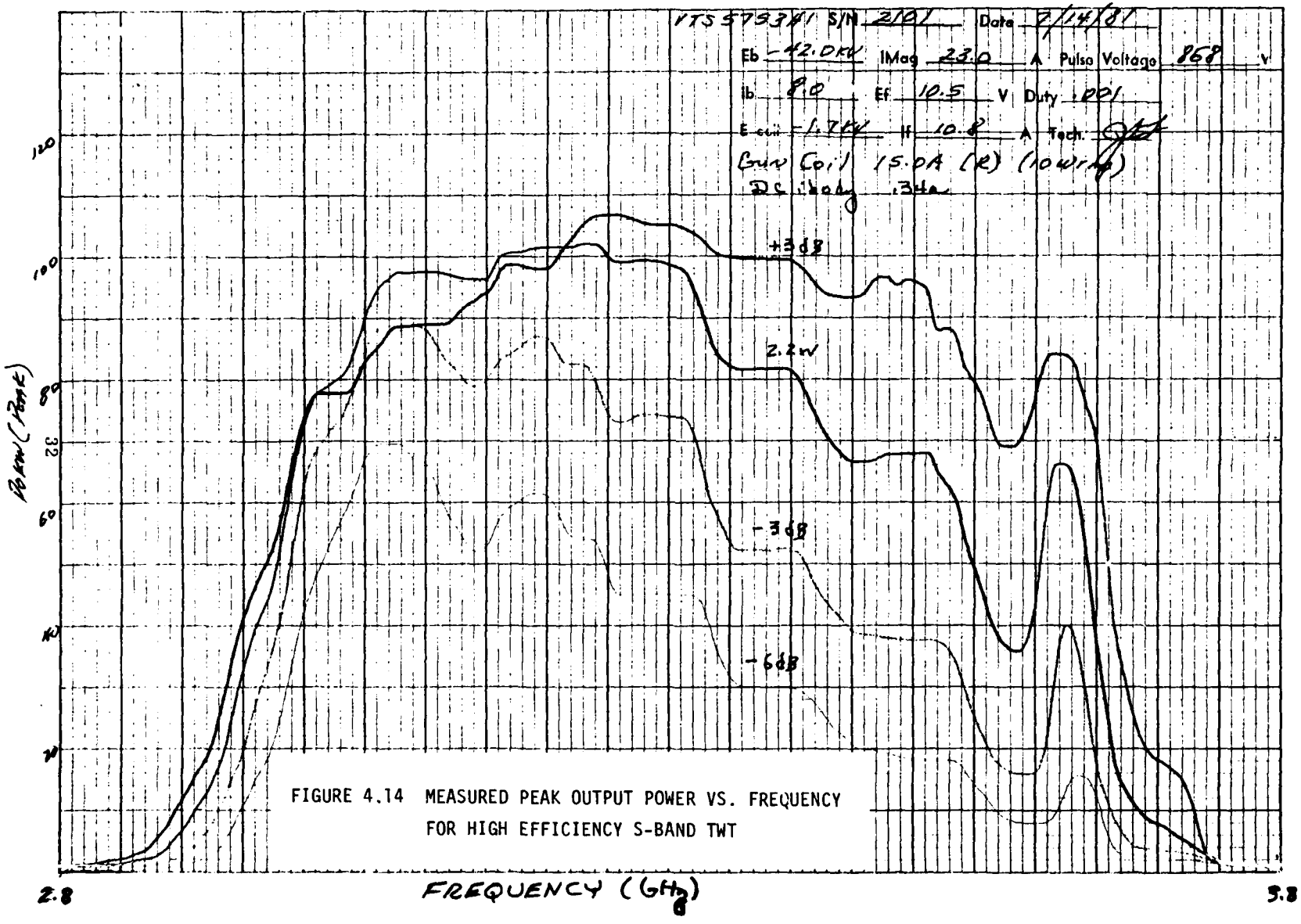

FIGURE 4.14 MEASURED PEAK OUTPUT POWER VS. FREQUENCY FOR HIGH EFFICIENCY S-BAND TWT

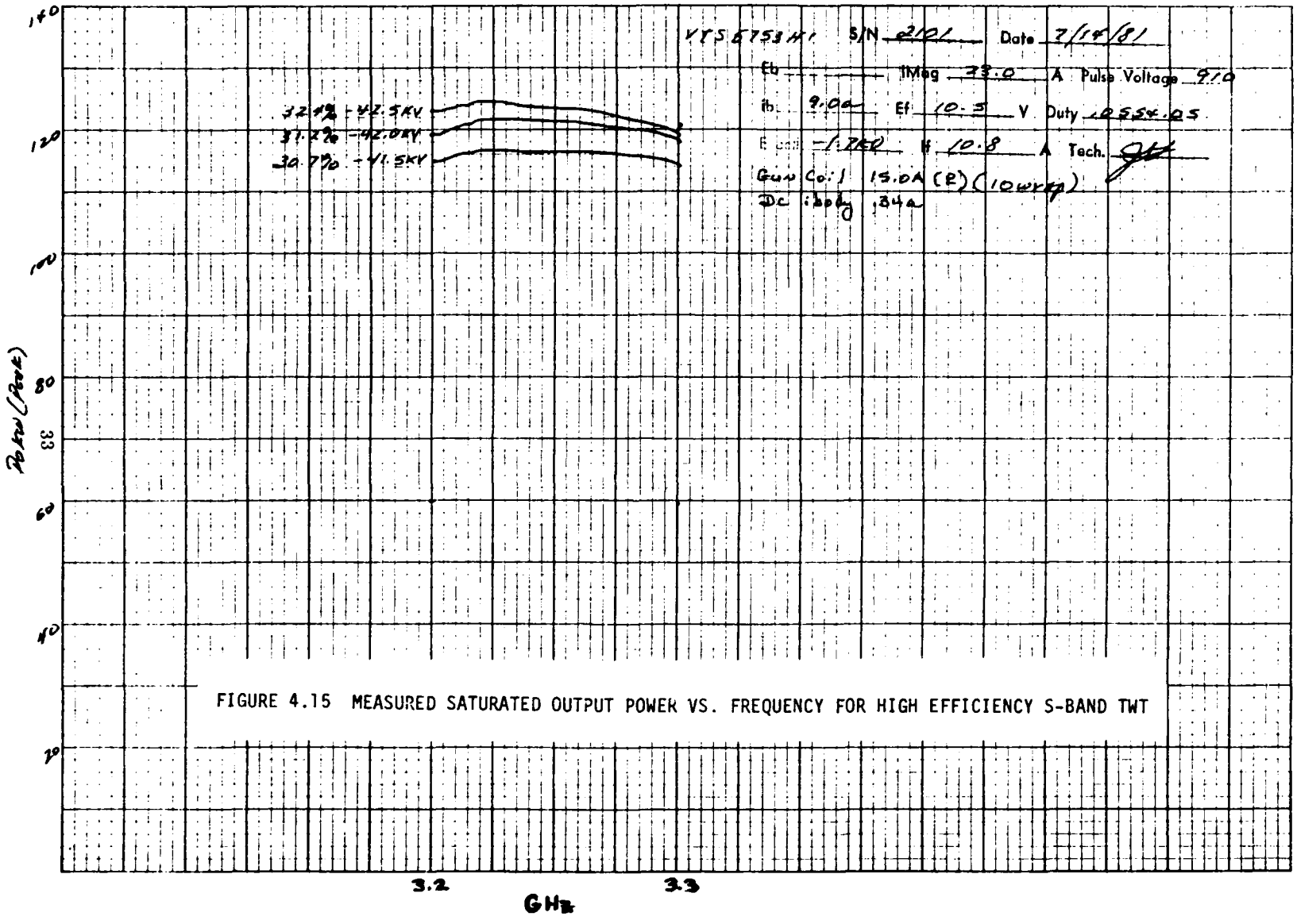

FIGURE 4.15 MEASURED SATURATED OUTPUT POWER VS. FREQUENCY FOR HIGH EFFICIENCY S-BAND TWT

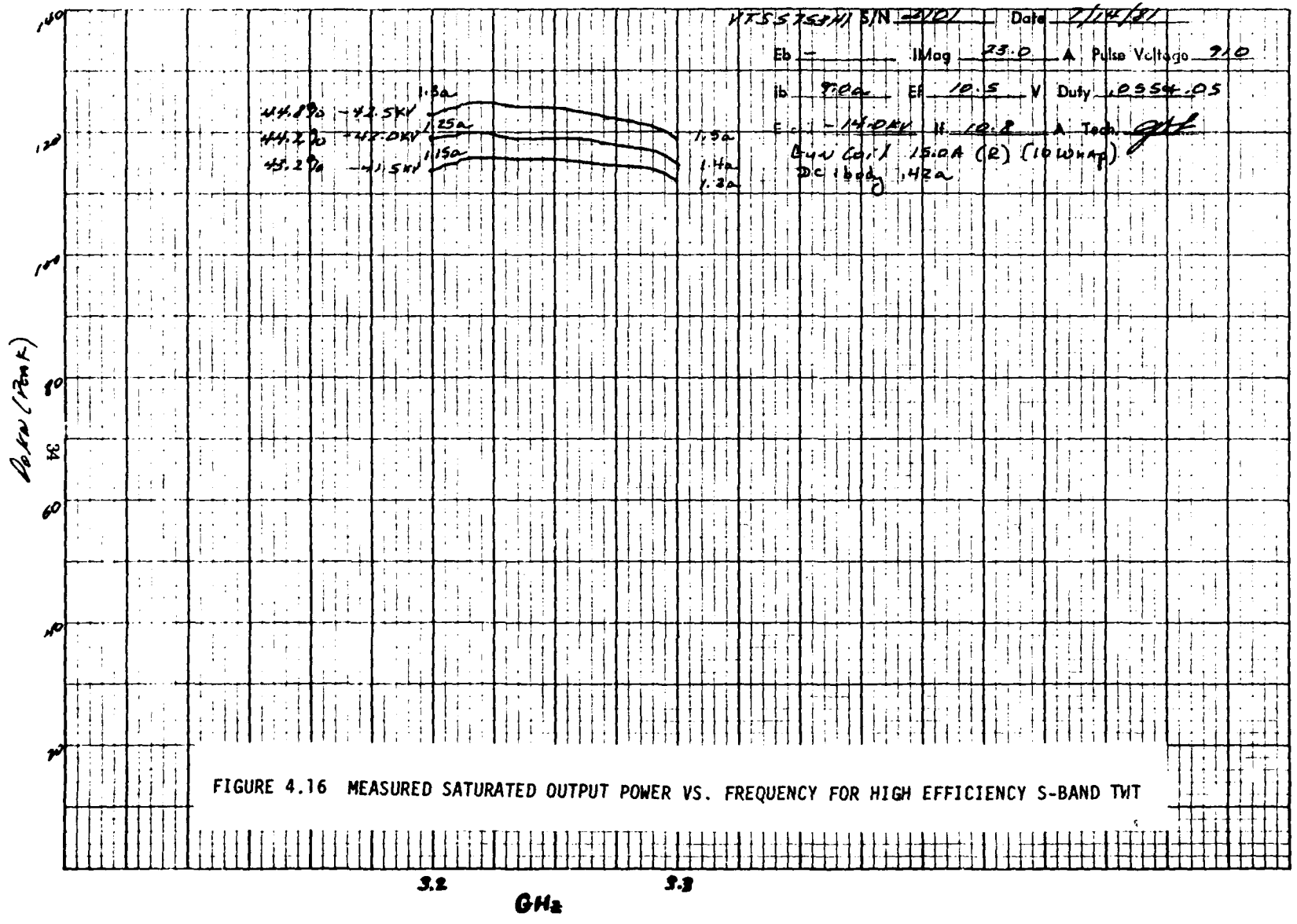

FIGURE 4.16 MEASURED SATURATED OUTPUT POWER VS. FREQUENCY FOR HIGH EFFICIENCY S-BAND TWT

Figures 4.17 and 4.18 show saturated power vs. frequency for operation at 42 KV and 9 A. The two sets of measurements are virtually identical, the former at 5.0 percent duty and the latter at 10% duty. The minimum saturated power is approximately 107 KW. The minimum average power is greater than 10 KW.

Figure 4.19 is a plot of measured start oscillation current vs. beam voltage. The predicted start oscillation current (Figure 3.4) is approximately 10 percent greater than the measured value. This correlation is considered excellent.

4.3 Analysis of Test Results

1. Frequency Band - Test results in Figure 4.11 show peak power greater than 100 KW over a 500 MHz band from 3.050 to 3.550 GHz. This band is slightly displaced from the objective 3.1 to 3.6 GHz band, but nevertheless represents proof of concept.

2. Electronic Bandwidth - The maximum measured peak power in Figures 4.11 is 122 KW. The minimum power is 108 KW. This represents a power flatness of ±0.25 dB.

3. Peak Power - The peak power specification of 100 KW has been met (Figure 4.11).

4. Average Power - The average power of 10 KW has been met (Figure 4.18).

5. Duty Factor - The experimental tube was operated up to a duty factor of 10%.

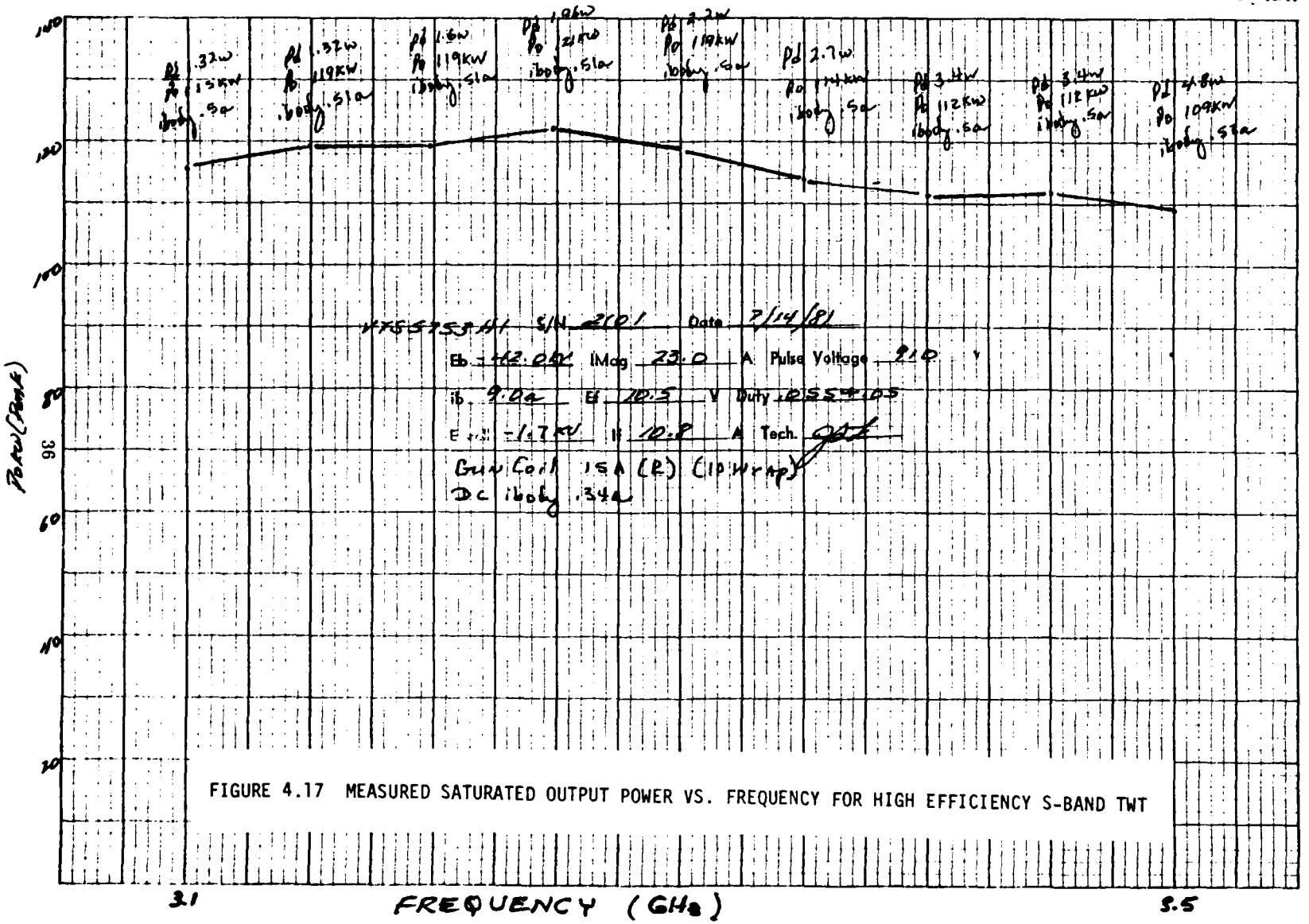

FIGURE 4.17 MEASURED SATURATED OUTPUT POWER VS. FREQUENCY FOR HIGH EFFICIENCY S-BAND TWT

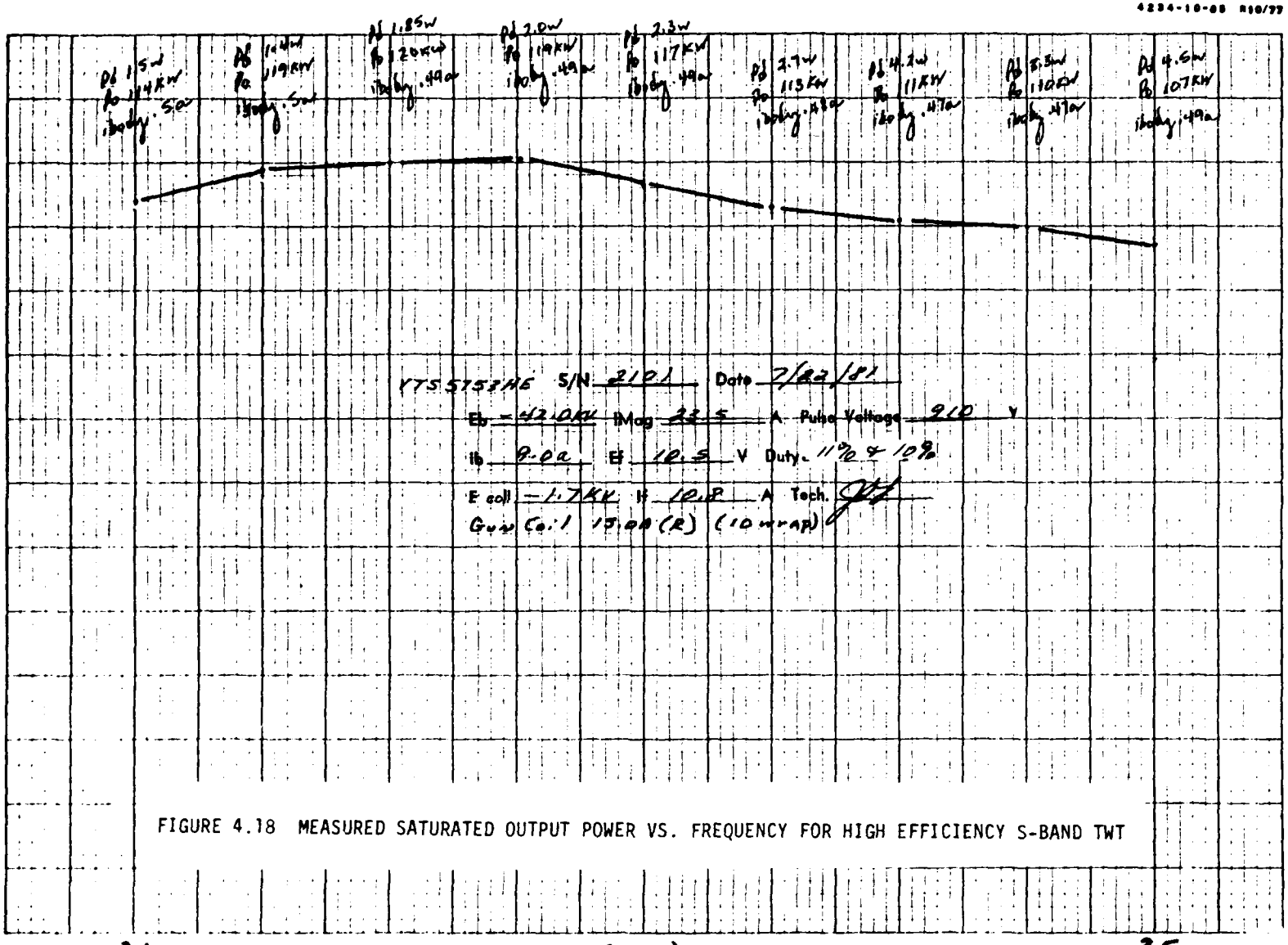

FIGURE 4.18 MEASURED SATURATED OUTPUT POWER VS. FREQUENCY FOR HIGH EFFICIENCY S-BAND TWT

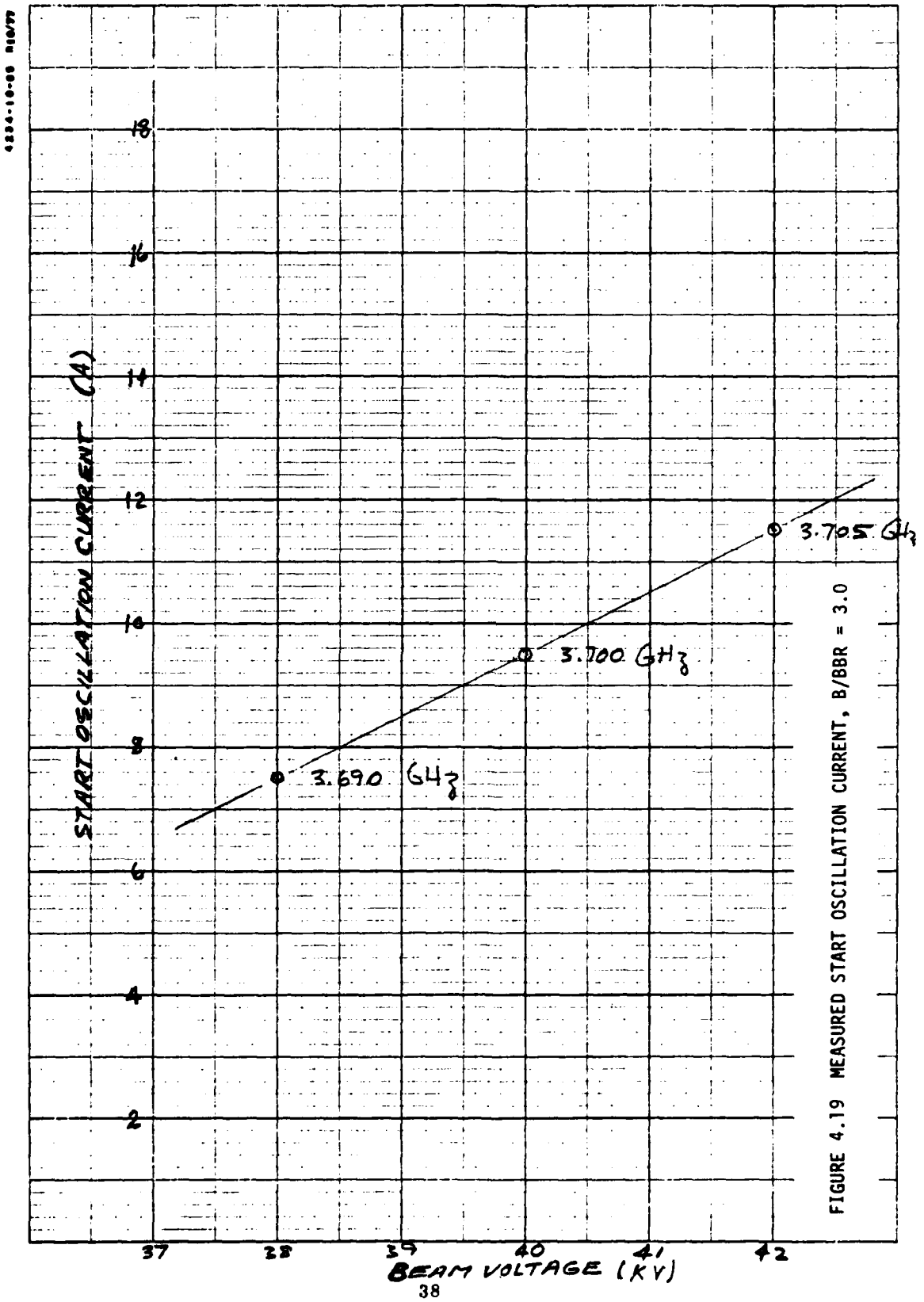

FIGURE 4.19 MEASURED START OSCILLATION CURRENT, B/BBR = 3.0

6. Pulse Width - This tube will operate at 10% duty at any pulse width up to 1 millisecond.

7. Gain - The saturated gain exceeds 40 dB (Figure 4.12).

8. Conversion Efficiency - The measured conversion efficiency at 3.2 GHz was 32.4% (Figure 4.15). This compares with a predicted efficiency under confined flow of 31.4%. The predicted efficiency under Brillouin focusing conditions is 43%.

4.4 Comparison of Computed and Measured Results

Figure 4.20 shows the experimentally measured small signal gain replotted from Figure 4.12 together with the computed small signal gain for the same case (V = 42 kV, I = 9.0 A, B/BBR = 3.0, b/a = 0.7). The fit is very good but can be slightly improved by increasing the beam voltage of the computer simulation to 44 kV. Figure 4.21 shows such a comparison.

Figure 4.22 shows the measured and computed saturated efficiency corresponding to the small signal example of Figure 4.20. The measured values are slightly better than the computed values. The accuracy of the agreement is very encouraging, and increases our confidence in the computer simulation.

Figure 4.23 shows computed efficiency vs. frequency for the same parameters employed in the measurement shown in Figure 4.15 (V = 42.5 kV, I = 9 A, B/BBR = 3.0). The measured efficiency at 3.2 GHz is 32.4 percent compared with a computed value of 31.4 percent. The measured efficiency takes account of the slight collector depression (1.7 kV). The actual conversion efficiency is 32.1 percent.

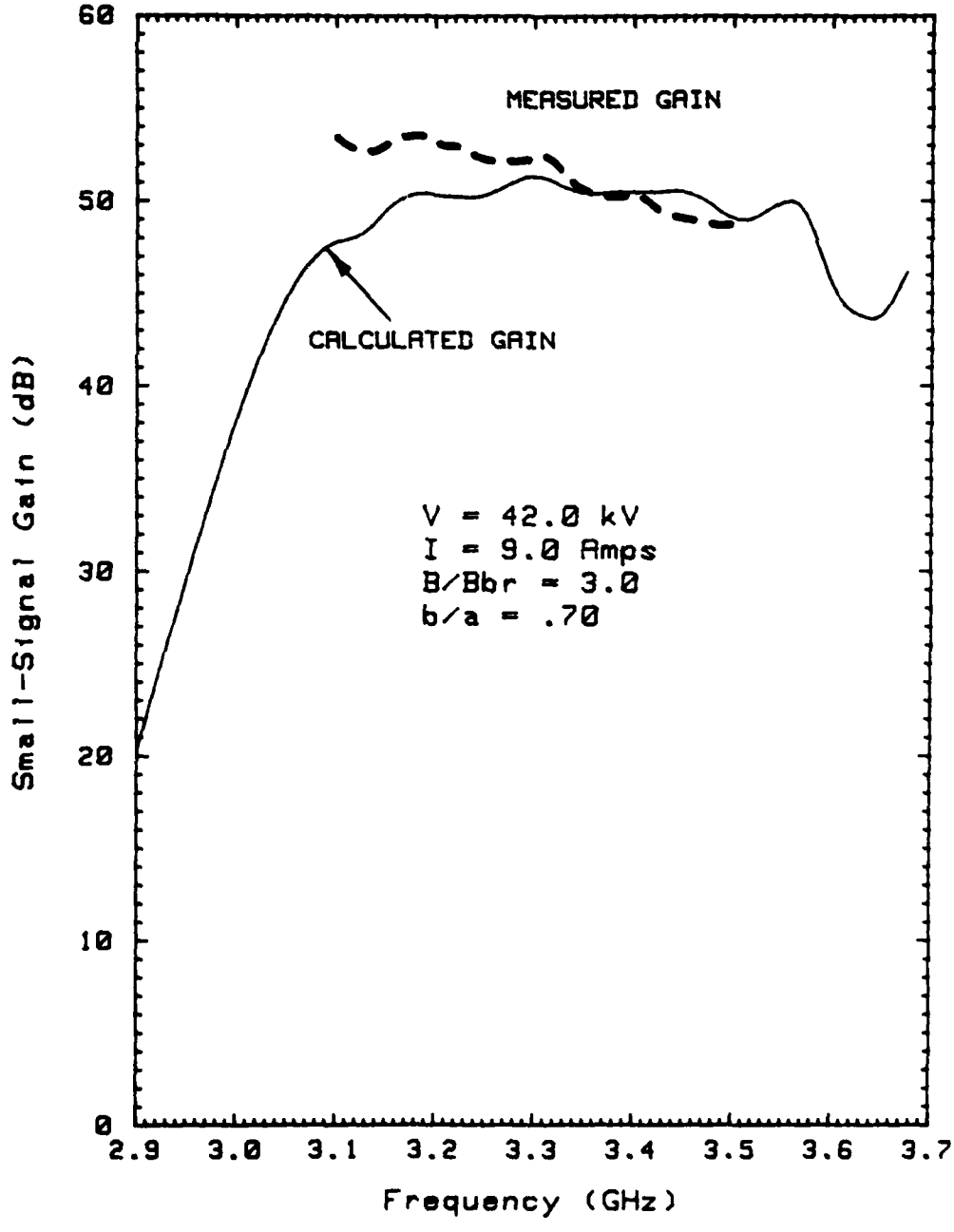

FIGURE 4.20 COMPARISON OF PREDICTED AND MEASURED SMALL SIGNAL GAIN FOR HIGH EFFICIENCY TWT

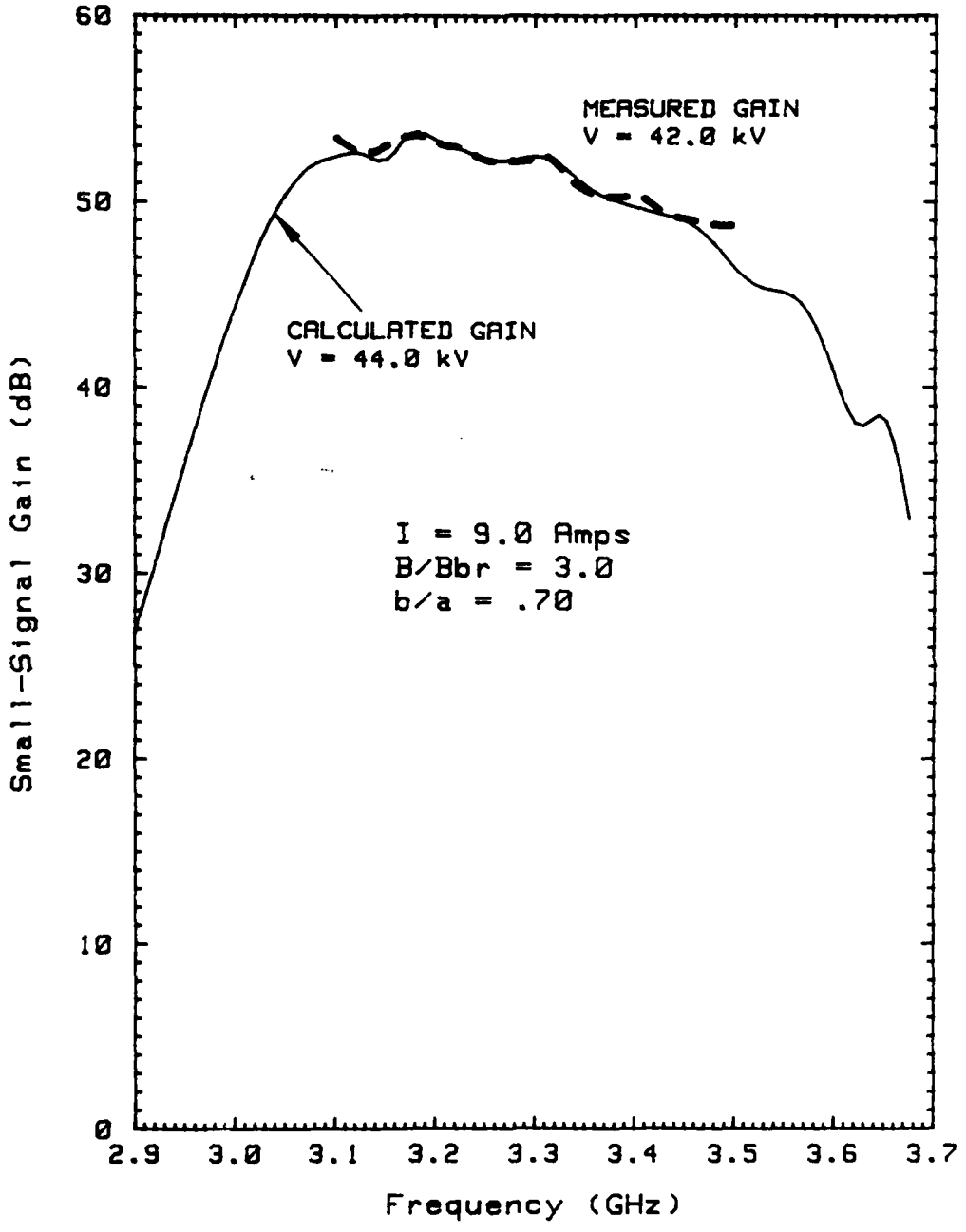

FIGURE 4.21 COMPARISON OF PREDICTED AND MEASURED SMALL SIGNAL GAIN FOR HIGH EFFICIENCY S-BAND TWT

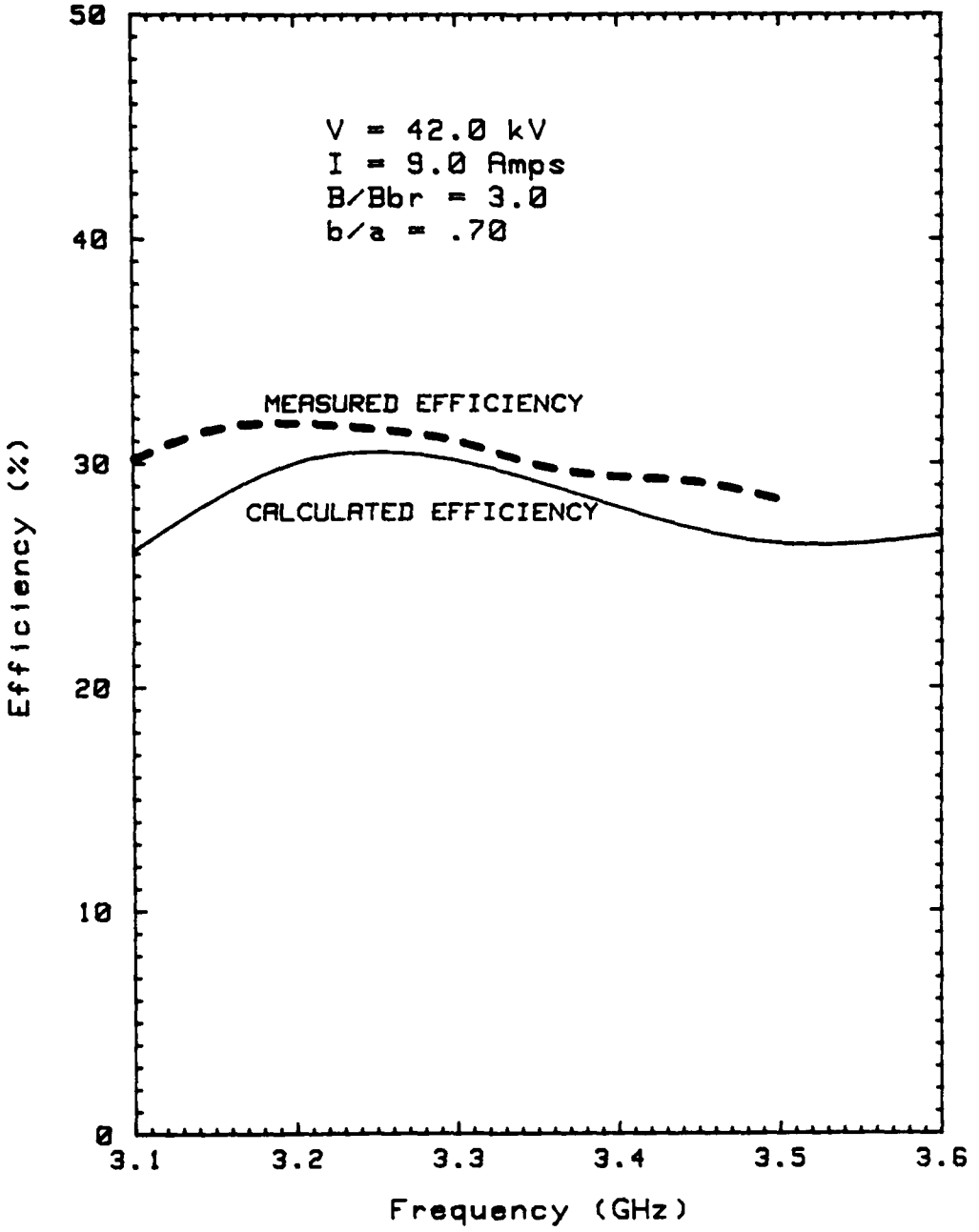

FIGURE 4.22 COMPARISON OF PREDICTED AND MEASURED CONVERSION EFFICIENCY FOR HIGH EFFICIENCY S-BAND TWT

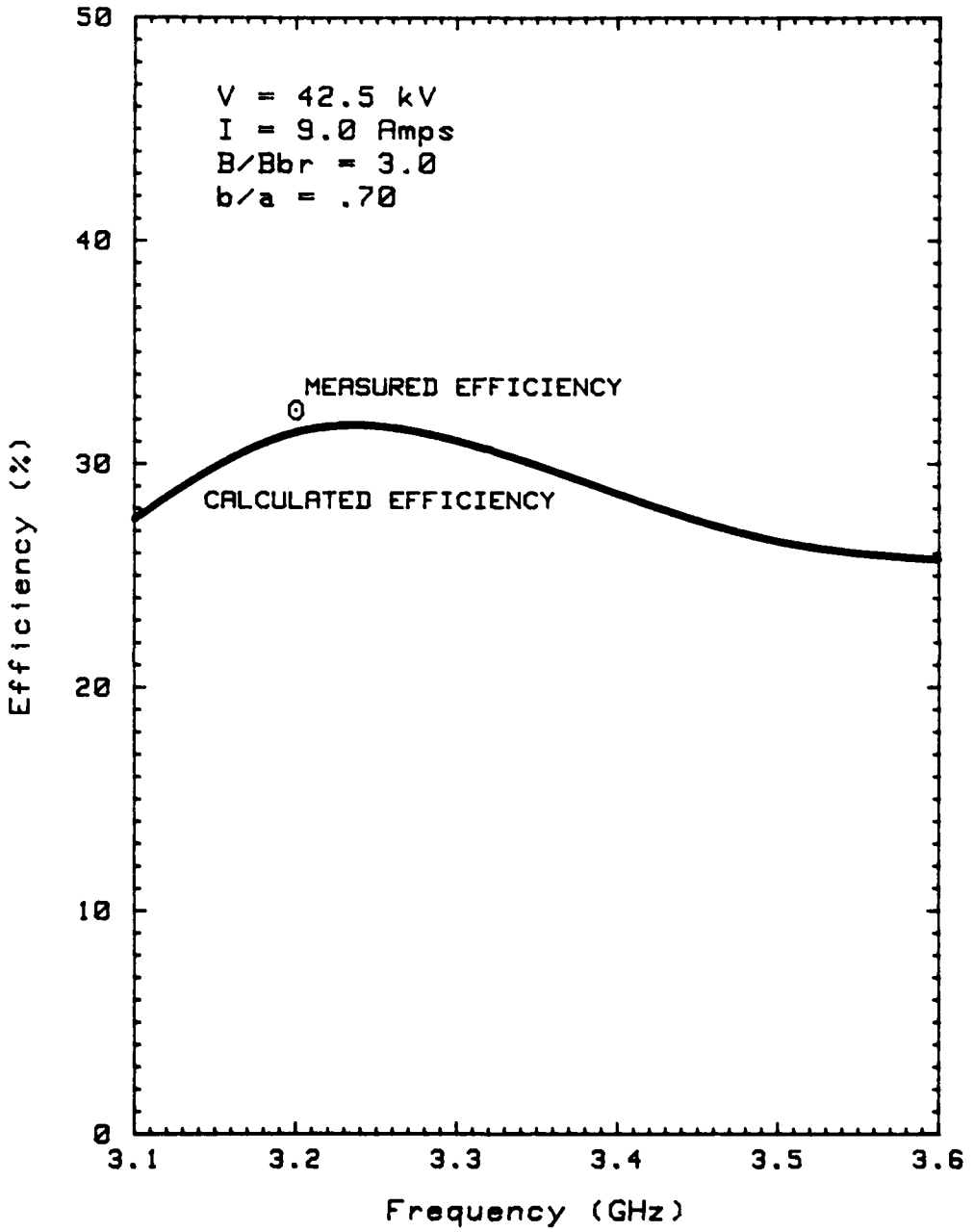

FIGURE 4.23 COMPARISON OF PREDICTED AND MEASURED CONVERSION EFFICIENCY FOR HIGH EFFICIENCY S BAND TWT

The agreement between theory and practice is good enough to justify extrapolating the computed results to the Brillouin beam case. Figure 4.24 shows the predicted efficiency for a tube employing a Brillouin beam with V = 42, I = 9, b/a = 0.70. The predicted efficiency is greater than 40 percent over approximately two-thirds of the band. By dropping the voltage to 40 KV the predicted efficiency becomes somewhat flatter and very nearly reaches the required 40 percent minimum efficiency over a full 500 MHz band. This result is plotted in Figure 4.25.

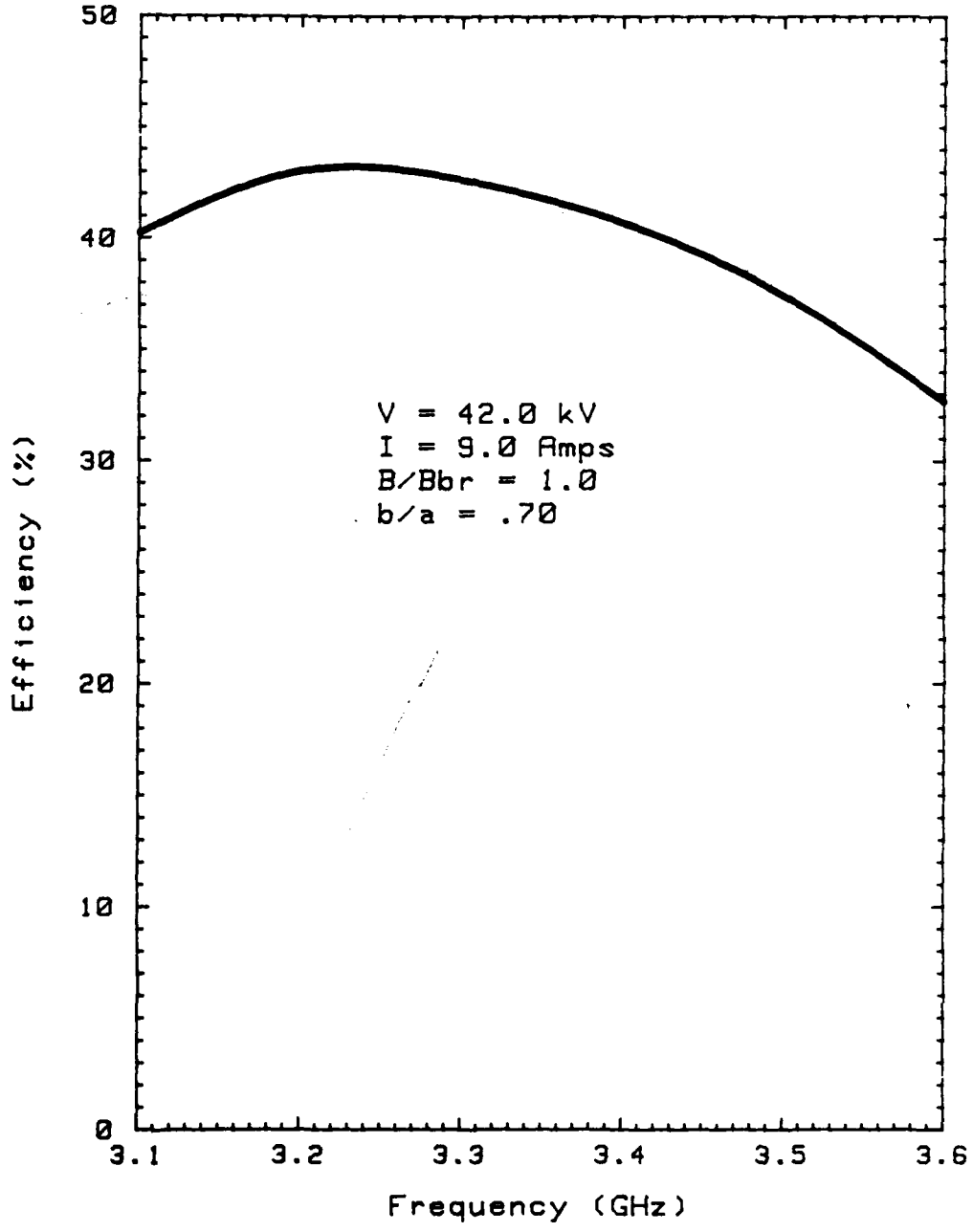

FIGURE 4.24 PREDICTED CONVERSION EFFICIENCY OF S-BAND TWT WITH BRILLOUIN BEAM

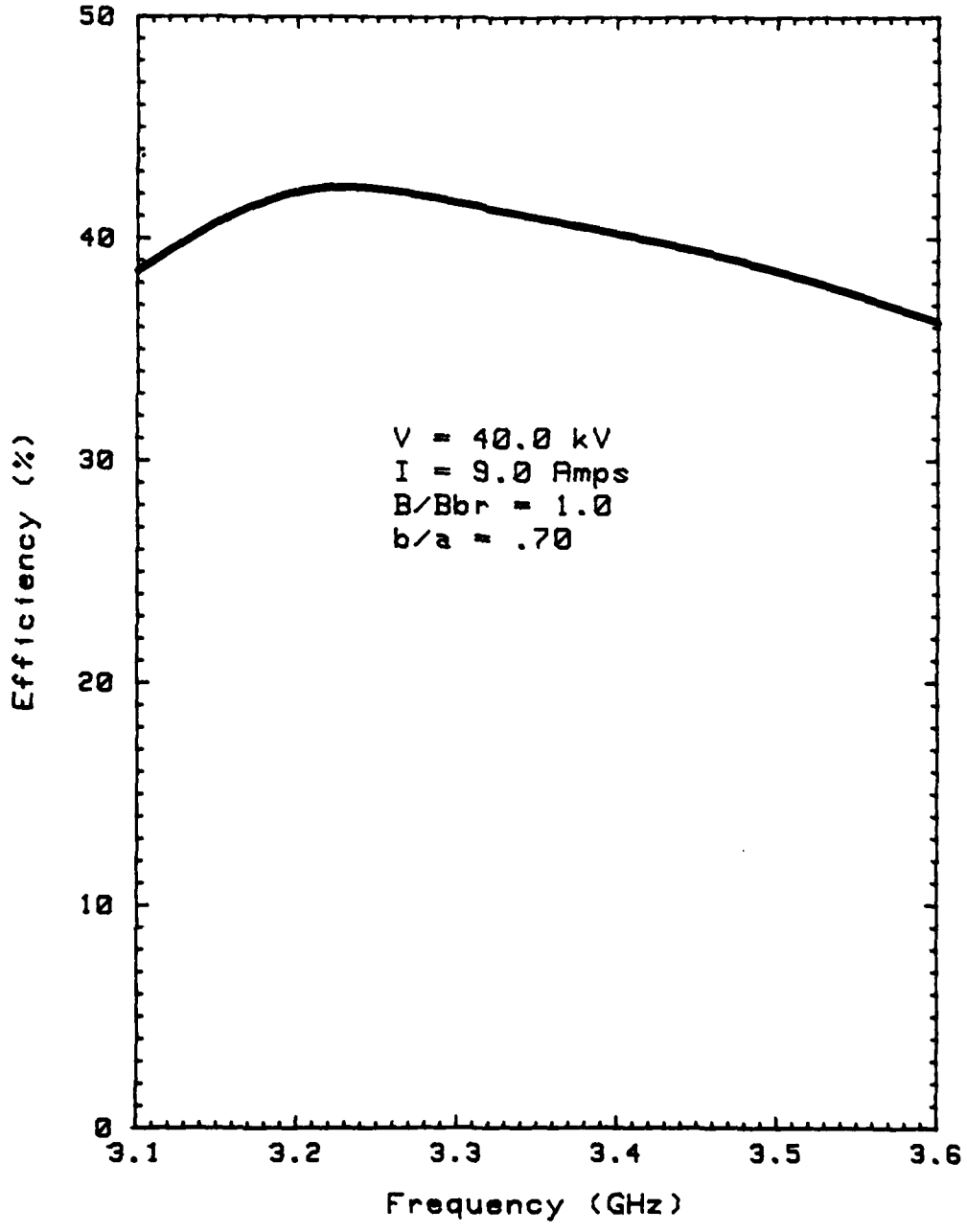

FIGURE 4.25 PREDICTED CONVERSION EFFICIENCY OF S-BAND TWT WITH BRILLOUIN BEAM

5.0 CONCLUSIONS AND RECOMMENDATIONS

This program to construct a tube to test the theoretical results of the preceeding study program was an unqualified success. Although the interaction efficiency was 8 percent less than that predicted by the theoretical study, it was the direct result of use of confined flow rather than a Brillouin focused electron beam. Further theoretical work predicted the identical 8 percent penalty due to substitution of the confined flow beam. This re-analysis was performed prior to hot testing of the vehicle.

The implications of the successful completion of this hardware phase is that the performance of a coupled cavity TWT can be predicted and in effect the tube can be designed on paper for any particular performance parameter desired--in this case, optimizing the efficiency while preserving the bandwidth and power handling capability.

The electronic efficiency enhancement achieved with a modest 33% depression of the existing single stage collector is very encouraging. This result implies that the velocity spread in the beam emerging from the output circuit is not greater than that of a tube with normal efficiency.

Our recommendation for future effort is that the development of the Brillouin focused electron gun be completed and the tube rebuilt in order to verify the originally predicted conversion efficiency of 40%.

The focus solenoid should also be redesigned to just provide the required Brillouin field with minimum weight size and power consumption. The existing confined flow solenoid weighs 200 pounds and consumes nearly 4 KW of power. Since shrinking the diameter of the solenoid reduces the magnetized volume by the square of the radius, impressive gains can be made in the weight of the coils and the iron return path as well as power consumption.

The next phase should also include improvement in the collector optics to optimize the energy recovery and maximize the overall efficiency.

MISSION
of
Rome Air Development Center

RADC plans and executes research, development, test and selected acquisition programs in support of Command, Control Communications and Intelligence (C^3I) activities. Technical and engineering support within areas of technical competence is provided to ESD Program Offices (POs) and other ESD elements. The principal technical mission areas are communications, electromagnetic guidance and control, surveillance of ground and aerospace objects, intelligence data collection and handling, information system technology, ionospheric propagation, solid state sciences, microwave physics and electronic reliability, maintainability and compatibility.


DATE
ILME